

**NATIONAL COOPERATIVE HIGHWAY RESEARCH PROGRAM
(NCHRP)**

**Project 01-57B: Validating Standard Definitions for
Comparable Pavement Cracking Data**

Task 8: Data Analysis

(Execute the Phase II Data Analysis Plan Approved in Task 6)

**PI: Yichang (James) Tsai, Ph.D., P.E.
Zhongyu Yang, Haolin Wang,
Trinh Flynt, Rahil Bhamani**

Georgia Institute of Technology

GGFGA Engineering, Inc.

Quality Engineering Solutions, Inc.

Table of Content

1	Overview of Task 8—Data Analysis.....	3
1.1	Objectives	3
1.2	Core Components in Validating the Cracking Definition.....	3
1.3	Research Approach.....	4
2	Feasibility Validation	5
2.1	Overview of the Process and Involved Algorithms for Reporting Revised WOD-288	5
2.2	Overview of Crack Reporting Items in Revised WOD-288	6
2.3	Detail Explanation of the Process and Algorithms	7
2.4	Case Study	15
2.5	Identified Challenges.....	24
2.6	Proposed Refinement.....	25
3	Sensitivity Analysis.....	26
3.1	Sensitivity Study of Grid Settings (Size and Location).....	27
3.2	Sensitivity Study of Crack Width Thresholds for Crack Severity Classification	28
3.3	Sensitivity Study of Crack Orientation Thresholds for Crack-type Classification.....	29
4	HPMS Reporting Using Revised WOD-288.....	30
4.1	HPMS Definition of Cracking Percentage Report.....	30
4.2	Methodology.....	31
4.3	Case Study	32
5	Validation of Proposed Cracking Data Quality Assessment Method	33
5.1	End-to-end Methods Validation.....	33
5.2	Decomposed Methods Validation	40
6	Conclusion.....	43
7	Appendix.....	45
7.1	Additional Results of Crack Width Distribution	45
7.2	Additional Results of Crack Orientation Distribution Analysis	47
8	References	49

1 Overview of Task 8—Data Analysis

Task 8 focuses on data analysis to execute the Phase II Data Analysis Plan approved in Task 6. This report is a preliminary document that will be further refined in the next task, Task 9, which involves preparing a final report presenting the results of the work plan.

1.1 Objectives

Data analysis in Task 8 using diverse data collected from different state highway agencies (SHAs) with different vendors and systems in Task 7 to achieve two main objectives in Phase II of this study:

- 1) **Objective 1: Validation and refinement of the revised WOD-288.** Task 8 aims to conduct data analysis to validate the feasibility of implementing the revised WOD-288, especially with the crack vector model (CVM), alligator cracking definition, and slab-based JPCP definition added. Challenges and potential issues will be identified through data analysis (including process development and use of algorithms) to suggest further refinement of the new cracking definition. A sensitivity study will be made to understand the impact of and validate parameters in the cracking definition, such as grid size, cracking width, and orientation thresholds. In addition, the use of revised WOD-288 in HPMS data reporting as an example will also be examined to validate the utility of the new cracking definition.
- 2) **Objective 2: Validation of the proposed cracking data quality assessment methods.** In this task, data collected in the field (i.e., Florida DOT trip in December 2024) is processed and analyzed to examine the feasibility of using the proposed methods and procedures to effectively assess cracking data quality under real-world conditions. This task focuses on analyzing ground reference data collected by two proposed ground referencing methods: a) manual surface crack mapping on engineering sheet, and b) manual crack augmentation on pavement surface.

1.2 Core Components in Validating the Cracking Definition

Three core components are identified during the data analysis for validating the revised WOD-288, which are 1) the cracking **definition**, 2) the **process** of reporting crack according to the definition, and 3) **algorithms** applied in the process of crack reporting. These specific terminologies are defined below as they will be used commonly in the following reports, and their relationships are important to understanding the proposed methodology for validating and refining the cracking definition.

- **Definition:** The cracking *definition* specifies the **rules, criteria, and standards** for identifying, measuring, and reporting cracks. It acts as the “rulebook” that ensures consistency across measurements.
- **Process:** The *process* refers to the **workflow steps** to implement the definition. Considering the revised WOD-288 is designed for automated cracking measurement systems, whether existing technologies are practical to implement the definition needs to be explored. This determines the feasibility of implementing the new cracking definition under the context of automated cracking measurement systems (not like the traditional definition designed for a human-based manual approach).

- **Algorithm:** *Algorithms* are the **specific computational methods** used to execute steps in the process. Under the context of applying automated distress evaluation systems, essential algorithms are needed to support the execution of the process for achieving the requirements specified in the definition. To validate and refine the proposed definition, examining essential algorithms and identifying potential issues and challenges is critical.

1.3 Research Approach

To achieve the two objectives mentioned in Section 1.1, the following research approaches are proposed and conducted.

- 1) **Validate the feasibility of implementing revised WOD-288 by developing *process* and running *algorithms* (Objective 1, Part 1):** To validate whether the revised WOD-288 is feasible to be implemented in the real-world environment, we developed the *process* and ran the *algorithms* to measure and report cracking using diverse data collected from different vendors and different systems. The goal is to assess whether a feasible process can be established and whether existing algorithms can be applied to automate crack reporting according to the revised WOD-288. The process developed and algorithms involved during the validation will be explained to provide insight into the breakdown steps for reporting cracking data using revised WOD-288. Essential information will be documented in the specification during the next tasks that ensure the revised WOD-288 can be effectively used by more SHAs and vendors.
- 2) **Identify challenges in implementing the revised WOD-288 and provide suggestions for further refinement (Objective 1, Part 2):** During the development of the *process* and application of *algorithms* for reporting cracking data according to the revised WOD-288 definition, the challenges and gaps of real-world implementation of the cracking definition are identified. Suggestions for further refinement of revised WOD-288 will be made, documented, and communicated with the panel. After discussion and approval by the panel, a second revised WOD-288 will be established.
- 3) **Conduct a sensitivity study to provide insights into parameters' impacts and thresholds in cracking definition (Objective 1, Part 3):** In addition to validating the feasibility, sensitivity studies have been conducted to provide insights into potential variations that parameters used in the revised WOD-288 can make. These parameters include a) grid size and position, b) crack width thresholds for severity classification, and c) crack orientation for crack type classification. The results will show i) the changes in cracking measurement with grid size and position changes and ii) the distribution of crack width and orientation. This information is critical to gaining insights into whether the existing parameters used in the revised WOD-288 can support consistent and reasonable cracking measurements. It is worth noting that many parameters were previously never examined using real-world cases, and this study is the first to conduct this level of analysis and validation.
- 4) **Exam the utility of revised WOD-288 by reporting HPMS cracking percentage (Objective 1, Part 4):** Revised WOD-288 is also designed to be flexible for supporting cracking reporting according to HPMS and agencies' specific cracking protocols. Thus, HPMS crack percentage reporting using revised WOD-288 is conducted to examine and demonstrate the flexible utility of revised WOD-288 for supporting and reporting other cracking protocols. Selecting HPMS reporting for the pilot study is used considering HPMS reporting is mandated for all SHAs. We are

collaborating with participating transportation agencies to demonstrate HPMS cracking reporting using the revised WOD-288, evaluating its utility and feasibility.

- 5) **Validate the proposed cracking data quality assessment methods (Objective 2):** This task aims to assess whether the proposed data quality assessment methods (i.e., *manual surface crack mapping (on engineering sheet)* and *manual crack augmentation (on pavement surface)* methods, described further in Section 5.1.) can be used effectively to evaluate cracking data quality—whether pavement images obtained from different vendors and sensing systems can be used to report and measure crack accurately and consistently in accordance with the revised crack definitions.

2 Feasibility Validation

This section conducts the research approaches (1) and (2) mentioned in Section 1.3, which are 1) validating the cracking definition by establishing process and running algorithms and 2) identifying challenges and providing refinement suggestions.

2.1 Overview of the Process and Involved Algorithms for Reporting Revised WOD-288

To provide an overview of the proposed process and the algorithms involved in reporting cracks based on the revised WOD-288, **Table 1** outlines the breakdown of steps, and the specific algorithms used in each step. The proposed process consists of eight steps, with essential algorithms introduced for some of them. It is important to note that asphalt and JPCP have different Level 2 and 3 reporting requirements. As a result, Steps 7 and 8 are divided into separate sections for asphalt and JPCP.

Table 1. Breakdown Steps and Involved Algorithms in Reporting Revised WOD-288

Steps	Description of the Step	Algorithm Involved
1	Pavement image data collection using imaging systems.	
2	Crack detection (e.g., crack segmentation).	Crack detection
3	Lane marking location identification	Lane marking detection
4	Crack map digitization for establishing the crack vector model (CVM)	Crack vector model computation
5	Link-wise crack attributes computation (i.e., crack length, crack width, crack location, crack orientation in degree, transverse or longitudinal crack, alligator crack or not, etc.)	
6	Level 1 link-wise crack reporting using crack vector model (CVM) in both crack map and tabular format	
7.1	Level 2 (asphalt) zone-wise crack reporting by aggregating link-wise crack information	Alligator crack classification
7.2	Level 2 (JPCP) slab-wise crack reporting	
8.1	Level 3 (asphalt) grid-based crack reporting	
8.2	Level 3 (JPCP) slab state reporting	Slab state classification

2.2 Overview of Crack Reporting Items in Revised WOD-288

During the development of the process for reporting revised WOD-288, we further clarified and refined the crack reporting items and their definitions for both asphalt and JPCP. For asphalt pavement, three levels of cracking information are reported as shown in **Table 2**; from fundamental to aggregated level information (i.e., fine-to-coarse), they are:

- 1) **Level 1 Link-wise** cracking information: Storing and reporting fine cracking information at the crack link level, where cracking attributes (e.g., length, average width, orientation) are measured for each individual piece of a crack link.
- 2) **Level 2 Zone-wise** cracking information: Reporting aggregated cracking attributes by different categories of cracking (i.e., transverse, longitudinal, alligator cracks) and different zones (i.e., wheelpath, non-wheelpath).
- 3) **Level 3 Grid-based** cracking information: The grid-based cracking report, outlined in WOD-288 definitions, involves quantifying pavement cracking by dividing the pavement surface into grids, typically 10 inches by 10 inches (250mm x 250mm) (Wang et al., 2020).

To clearly specify the reporting items, we added a reporting number for each item, such as “3.1 Percentage of Cracks” under grid-based cracking information, and “2.1 Length of Non-wheel Path Longitudinal Crack” under zone-wise cracking information.

Table 2. Reporting Items in Revised WOD-288 (Asphalt)

Levels	Reporting Items	Item Description/Definition	Severity Level	Min. Length	Orientation	Unit
Lv. 3 (Grid-based)	3.1 Percentage of Cracks	Percentage of grids having cracks (grid size of 250 mm by 250 mm)				%
	3.2 Percentage of Cracks by Severity Levels	Further break down item 3.1 into three severity levels according to crack width.	L (< 6 mm) M (6~12 mm) H (> 12 mm)			% % %
	3.3 Percentage of Wheel-path Cracks	Highlight cracks within the wheel paths from all detected cracks.				%
Lv. 2 (Zone-wise)	2.1 Length of Non-wheel Path Longitudinal Cracks	Length of longitudinal cracks in zones 1, 3, and 5, defined by a crack orientation between 0° and 20° and a minimum length of 12 inches.	L M H	12 in. (end point to end point)	0° ≤ α < 20°	ft. ft. ft.
	2.2 Length of Transverse Cracks	Length of transverse cracks, which must span at least two zones with an orientation between 70° and 90°. A zone is considered spanned if the crack covers more than 50% of its width.	L M H		70° < α ≤ 90°	ft. ft. ft.
	2.3 Length of Wheel Path Cracks	Total length of cracks in zones 2 and 4, including all types (e.g., alligator cracks), must be a minimum of 12 inches.	L M H	12 in. (end point to end point)		ft. ft. ft.
	2.4 Area of Alligator Cracks	The area of alligator cracking is determined by multiplying the approximate length of the affected area by the width of the wheel path zone. Items 2.2 and 2.5 are excluded from this calculation.				ft. ²
	2.5 Length Sealed Cracks	Length of sealed cracks refers to any crack that has been treated with a sealant material.				ft.
	2.6 Length of Other Cracks	Length of other cracks includes all cracks in zones 1, 3, and 5 that are not covered in items 2.1 and 2.2.				ft.
Lv. 1 (Link-wise)	1 Crack Vector Model (CVM)					

For JPCP, three levels of reporting items are listed in **Table 3**. Level 1 is the same as asphalt, the crack vector model (CVM). Level 2 reports cracking information (e.g., number of crack intersections, total crack length, average crack width) by crack types (i.e., longitudinal and transverse). Level 3 reports slab state based on crack pattern following a modified LTPP JPCP slab state definition. The smallest reporting unit for JPCP is one slab. Thus, all Levels 1-3 will be reported for each slab.

Table 3. Reporting Items in Revised WOD-288 (for JPCP)

Levels	Reporting Items		Unit
Level 3 (Slab State)	3 Slab state based on cracking pattern		Modified LTPP slab state based on cracking pattern: NC, L1, L2, T1, T2, CC, SS
Level 2 (Slab-wise)	2.1 Slab with or without crack	Yes or No: Y=1/N=0	
		Count of Cracking Intersections	#
	2.2 Longitudinal crack	Total Length	mm
		Representative/Average Width	mm
	2.3 Transverse crack	Total Length	mm
		Representative/Average Width	mm
Level 1 (Link-wise)	2.4 Other	Total Length	mm
		Representative/Average Width	mm
Level 1 (Link-wise)	1 Crack Vector Model (CVM)		

2.3 Detail Explanation of the Process and Algorithms

This section introduces more details of the proposed process and involved algorithms for reporting crack data based on the revised WOD-288. These involved algorithms were previously developed by the GT research team; most of these algorithms have alternative programs available from open-sourced coding packages, or they can be reimplemented based on the descriptions.

2.3.1 Step 1: Pavement Image Data Collection

Revised WOD-288 is designed for automated pavement cracking measurement and reporting based on pavement imaging systems. Thus, we assume all users of the revised WOD-288 will collect pavement images in accordance with the appropriate AASHTO Standards (e.g., PP 121, Acceptance of Ground Reference Scanning Equipment for Pavement Imaging System Assessment) as their first step.

2.3.2 Step 2: Crack Map Detection

This step aims to detect crack maps automatically from pavement range images. In this project, we use a deep learning-based crack segmentation (i.e., pixel-level crack detection) model previously developed by our research team (Hsieh, 2023; Hsieh & Tsai, 2020). Crack segmentation masks are normally binary images, in which “1” represents crack objects and “0” represents the background. Therefore, most of the pixels in segmentation images are black except for a few pixels which represent pavement cracks. **Figure 1** shows an example of a pavement range image with its corresponding segmentation result. The detected crack segmentation is used to generate crack maps in the following steps.

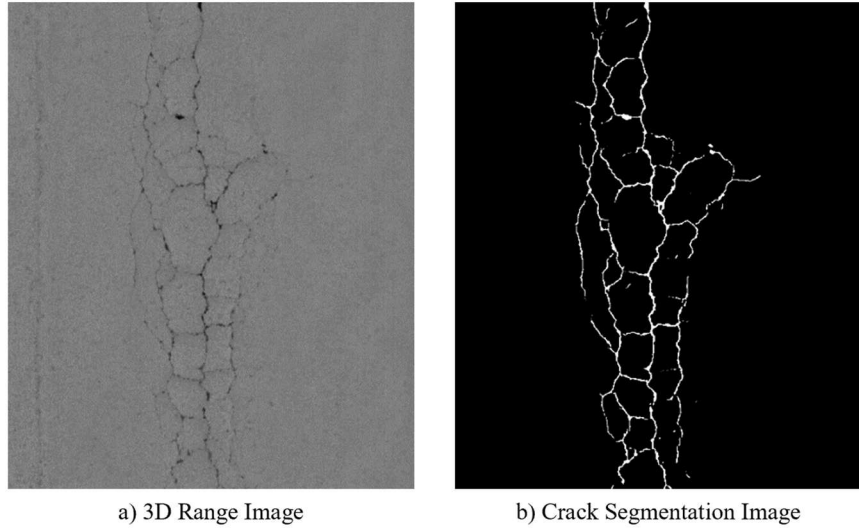
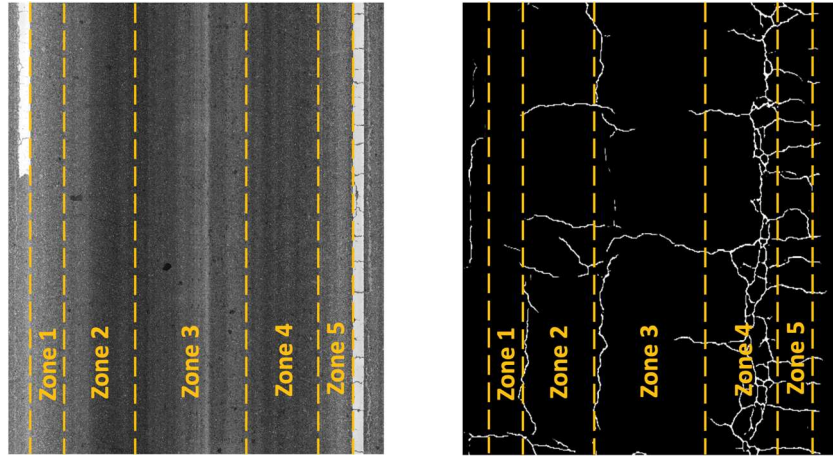


Figure 1. An Example of a 3D Range Image and its Corresponding Crack Detection (Hsieh, 2023; Hsieh & Tsai, 2020; Yang, 2024)

2.3.3 Step 3: Lane Marking Detection and Zone Generation

Knowing the cracking location related to the lane marking and wheel paths is essential for determining cracking types for not only revised WOD-288 but also HPMS and agencies' protocols. The lane marking detection is developed based on the Haugh transform algorithm and applied to the 2D intensity image. With the lane marking location identified, zone locations are computed according to the WOD-288 definition (Wang et al., 2020).

The pavement center is determined based on lane markings (midpoint if both are detected, 6 ft or half-lane width if one is detected, or image center if none are detected). Zones are then defined: Zone 3 is a 30-inch median centered on the pavement center, flanked by 40-inch wheel paths (Zones 2 and 4), with the remaining areas within the lane markings designated as Zones 1 and 5. Zone boundaries are calculated outward from Zone 3 until reaching lane markings or image edges. The actual width of wheel paths may be slightly adjusted in the implementation stage, according to the width of the lane (e.g., using 39-inch instead of 40-inch for a narrower 11 ft wide road). The following **Figure 2** shows the computed zone locations overlaid on the intensity and crack map.



(a) Zone Overlay on Intensity Image (b) Zone Overlay on Crack Map
Figure 2. Illustration of Lane Marking Detection and Zone Generation.

2.3.4 Step 4: Crack Vector Model (CVM) Establishment

The CVM generation algorithm is developed and applied to the pair of pavement range images and crack maps. The crack map is vectorized into a fundamental combination of links and nodes. The crack information is extracted including the length, width, orientation, and position of each fundamental component, as illustrated in **Figure 3**. More detailed step-by-step explanations for creating CVM can be found in Dr. Zhongyu Yang's PhD dissertation (Yang, 2024).

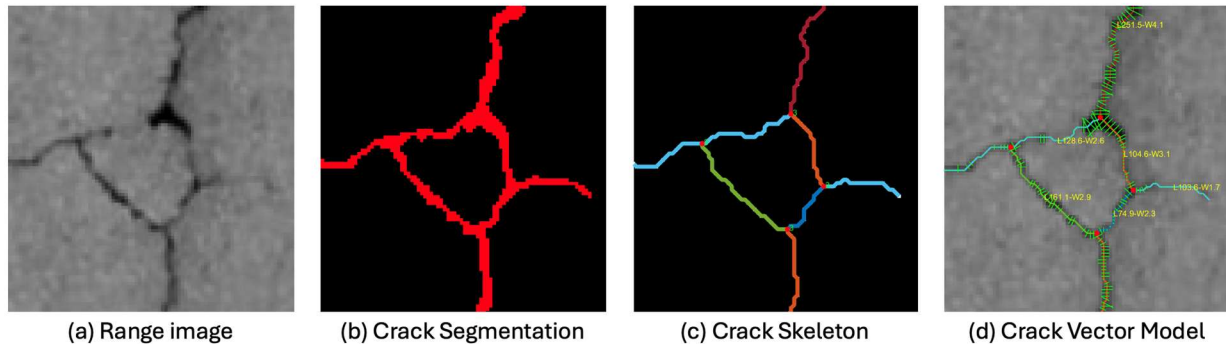


Figure 3. Illustration of Result CVM and Measurement Using the Developed Model (Yang, 2024).

2.3.5 Step 5: Link-wise Crack Attributes Computation

After crack vector model (CVM) is established, cracking attributes for each crack link can be calculated, such as 1) crack length, 2) average crack width, 3) cracking severity based on crack width, 4) crack orientation, 5) cracking type based on crack orientation (i.e., transverse, longitudinal), 6) cracking position (e.g., zone 1, zone 2: left wheelpath, zone 3, zone 4: right wheelpath, zone 5), and 7) cracking type based on cracking density (i.e., alligator/fatigue crack). This is the information derived from CVM which is to be reported in the Level 1 link-wise crack information reporting. The methods for computing this information from CVM are straightforward, such as accumulating coordinates for total crack length, more details can be found in Dr. Zhongyu Yang's PhD dissertation (Yang, 2024).

2.3.6 Step 6: Level 1 Link-wise Cracking Information Reporting

This level outlines the essential crack attributes extracted from typical crack maps generated by vendors or systems analyzing pavement images. It includes the crack features—nodes and links—and their attributes (length, width, orientation, and position), which together form the Crack Vector Model (CVM). This standardized format enables efficient storage of CVM data and facilitates a smoother transformation into higher-level, aggregated crack definitions.

The CVM features and properties are generated and exported in the format shown in **Table 4**, consolidating CVM links and nodes into a comprehensive representation of crack maps. Columns S2-S6 are essential information that can be used to re-establish the CVM, and they can be used to derive information in S7-S11. This derived information is essential for supporting the cracking report at the next level, such as the cracking location for determining wheel path crack or non-wheel path crack. The definitions of each column in **Table 4** are listed below:

- **S1:** Unique ID for each crack map (image)
- **S2:** Lane marking information for each crack map (image)
- **S3:** Unique ID for each crack link
- **S4:** X-Y coordinates of all continuous pixels along a crack link
- **S5:** Crack width (in mm)
- **S6:** Sealed crack indicator (1 for sealed, 0 otherwise)
- **S7:** Representative (average) crack width (in mm)
- **S8:** Severity level is determined by the representative crack width, i.e., Low: < 6 mm; Medium: 6-12 mm; and High: > 12 mm.
- **S9:** Length of a crack link (in mm)
- **S10:** Angle (in degrees) between the crack link direction and travel direction, ranging from 0° to 90° clockwise
- **S11:** Zone classification for the crack link, plus the percentage of its length within each zone. For example, “[$(2, 0.83), (3, 0.17)$]” means 83% of the crack is in Zone 2, and 17% is in Zone 3.
- **S12:** Alligator crack indicator (1 if a crack link belongs to alligator cracking)

It is noted that the CVM table for JCPC is very similar to Asphalt, while the differences are: 1) the “Slab ID” is added after “Image ID” because JPCP is based on slab-wise reporting; and 2) “S2, Zone Position”, S11 Position, and S12 Alligator Crack are not in the JPCP.

Table 4. Level 1 Link-wise Crack Reporting Generated by CVM (Asphalt).

Image ID	Zone Position (lane marking)	Link ID	Geometry	Width (mm)	Sealed Crack	Representative/Average Crack Width* (mm)	Severity Level*	Length* (mm)	Orientation* (deg)	Position* (zone, ratio)	Alligator Crack*
S1	S2	S3	S4	S5	S6	S7*	S8*	S9*	S10*	S11*	S12*
1	zone1_left_px=z1 zone2_left_px=z2 zone3_left_px=z3 zone3_right_px=z3r zone4_right_px=z4 zone5_right_px=z5	1	[(x11, y11), (x12, y12), ..., (x1n, y1n)]	(w11, w12, ..., w1n)	0						
		2	[(x21, y21), (x22, y22), ..., (x2m, y2m)]	(w21, w22, ..., w2m)	1						

* Information derived from the essential columns (S7-S11 are columns derived from S2-S6).

2.3.7 Step 7.1: Level 2 (Asphalt) Zone-wise Reporting

This level reports cracking attributes/properties (e.g., crack length, width, area) by different categories of cracking (i.e., transverse, longitudinal, alligator cracks) under different zones (e.g., wheelpath, non-wheelpath) through aggregating link-wise information extracted from CVM. The following components are considered for reporting Level 2 cracking information.

- **Component 1: Zone-wise Crack Length Calculating**

Crack links will be split when they pass through the boundary of a zone, and they will be aggregated for where the piece of crack is located. Using the crack position data (column S11) from the CVM table, the zone-based length of each crack link is calculated by multiplying the total length (column S9) by the percentage in each zone. Zones 2 and 4 are wheel path zones, while Zones 1, 3, or 5 are non-wheel path zones.

- **Component 2: Crack Width-based Severity Classification**

Crack width can vary along its length, a representative crack width (Wr) is needed for consistent reporting. WOD-288 initially recommended using the average width, but following panel discussions, percentile-based measurements (such as the 85th percentile) are now also considered. Agencies and vendors may choose a preferred representative width based on their standard practices. Crack severity can also be customized and is classified by Wr as a) Low: < 6 mm, b) Medium: 6–12 mm, and c) High: > 12 mm. Sensitivity study conducted in the next section aims to verify whether the existing thresholds are appropriate or not.

- **Component 3: Crack Type Classification**

Each crack in the CVM is categorized according to the revised crack definition, using properties like length, orientation, and position. **Table 5** presents criteria for classifying cracks by type. After classification, crack types are recorded as an additional attribute to the original CVM table.

The current definition has two challenges to be addressed: 1) these crack types are not mutually exclusive (i.e. a crack can be sealed and transverse); 2) the discontinuity of the crack, which is caused by either missing cracking detection or cracking bifurcation. We will summarize these issues and make suggestions in the next stage to address potential issues.

Table 5. Classification Criteria for Asphalt Pavement Crack Type

Crack Type	Description	Min. Length	Orientation	Position
Non-wheel Path Longitudinal Cracks	Crack links located in Zones 1, 3 and 5 with orientations ranging from 0° to 20° and a minimum length of 12 inches.	12 in. (end point to end point)	0° ≤ α < 20°	Zones 1, 3, 5
Transverse Cracks	Crack links with orientations ranging from 70° to 90° and span at least two zones. A zone is considered spanned if the crack covers more than 50% of the its width.		70° < α ≤ 90°	All zones
Wheel Path Cracks	Crack links in Zones 2 and 4, including all types (e.g., alligator cracks), must be a minimum of 12 inches.	12 in. (end point to end point)		Zones 2 and 4
Alligator Cracks	Crack links that satisfy the established thresholds for intersection density, crack branch count, and average crack length. This definition will be revised if a more reliable algorithm is developed.			Zones 2 and 4
Sealed Cracks	Crack links that has been treated with a sealant material.			All zones
Other Cracks	Crack links in Zones 1, 3, and 5 that are not classified as non-wheel path longitudinal or transverse cracks.			Zones 1, 3, 5

The above-mentioned cracking types can be straightforwardly differentiated using simple criteria and CVM, except alligator cracking. In this study, a simple method has been developed to classify alligator/fatigue cracks based on cracking density. It is worth noting that this simple model was developed only based on a small dataset; it has significant potential to further fine-tune this model.

The results of whether a crack link belongs to alligator cracking have been recorded in column S12 in the CVM table. **Figure 4(c)** shows an example of alligator cracking classified where alligator cracks are marked in red. **Figure 4(b)** is the corresponding CVM result used for classifying alligator cracks in which different color represents an individual crack link. It is worth noting that the alligator classification model used in this study is a simple approach we developed to demonstrate the feasibility of using CVM for classifying alligator cracks. Machine and Deep Learning-based models have great potential to achieve better results using pavement range images or crack segmentation directly. However, developing an accurate alligator cracking classification model is beyond the scope of this study; this alligator identification method is also used in Section 4.2 to identify fatigue crack for HPMS reporting.

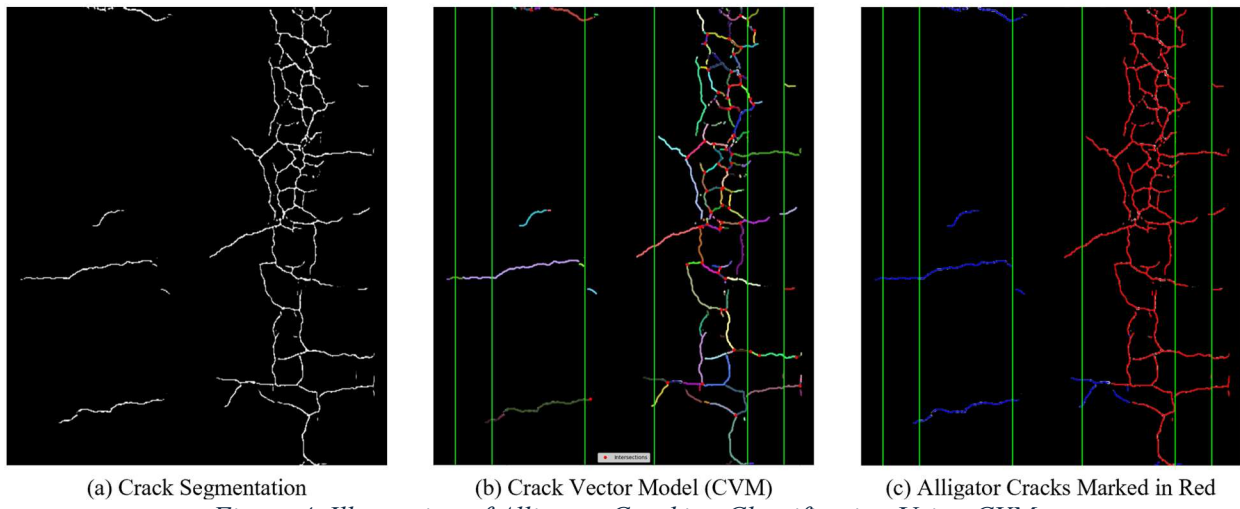


Figure 4. Illustration of Alligator Cracking Classification Using CVM

After alligator cracks are identified, based on the current definition (Section 4.2), the area of alligator cracks is calculated by multiplying the length of the affected area in both wheel paths and the width of the wheel path, as described in **Eq. 1**. A limitation of the current method related to the lack of consideration of the lateral extent of alligator cracking has been identified and is discussed in Section 2.5.3.

$$A = (L_1 + L_2) \times W \quad Eq. 1$$

Where **A** denotes alligator cracking area, **L₁** denotes the length of the affected area on the left wheel path, **L₂** denotes the length of the affected area on the right wheel path, **W** denotes the width of a wheel path zone, which is typically 40 inches.

2.3.8 Step 7.2: Level 2 (JPCP) Slab-wise Crack Reporting

For JPCP, in Level 2, cracking information is aggregated and reported for each slab, which is named “slab-wise crack reporting.” For each slab, whether this slab has any crack or not is first checked. Then, the number of cracking intersections is extracted from CVM. It is noted that the cracking bifurcation and discontinuity may impact the count of cracking intersections. The original design for counting cracking

intersections is to support determining the crack state, while it has been found challenging to determine the ideal number of cracking intersections.

After that, longitudinal and transverse cracks are differentiated for aggregating their total crack length and average crack width. The criteria for determining longitudinal or transverse is the same as asphalt: 0-20 degrees for longitudinal crack and 70-90 degrees for transverse crack.

2.3.9 Step 8.1: Level 3 (Asphalt) Grid-based Crack Reporting

For asphalt pavement, in Level 3, grid-based crack reporting is outlined in WOD-288 and involves quantifying pavement cracking by dividing the pavement surface into grids, typically 10 inches by 10 inches (250mm × 250mm). The process is as follows:

- **Gridline generation and placement:** The gridline with a grid size of 250mm by 250mm is first generated, and it is overlaid with the pavement image by aligning the center of the gridline with the center of the left and right lane marking positions. An example of a gridline overlaid on the crack map is shown in the **Figure 5**; red grids are the ones with cracks identified.

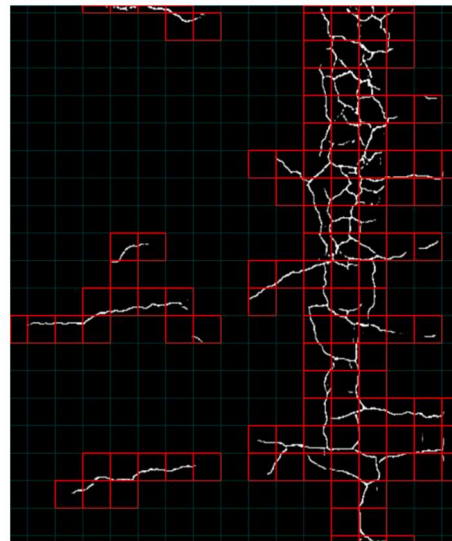


Figure 5. Illustration of Generated Grid Overlaying on Crack Map.

- **Cracked vs. Non-Cracked Grid Classification:** Examine each grid to determine if it intersects with any crack, even by a single pixel. If it does, classify it as a cracked grid; otherwise, label it as non-cracked.
- **Cracked Grid Severity Classification:** For each grid with cracks, assign a single representative width value based on the crack widths within the grid. Then, categorize each grid into a severity level based on the representative crack width (i.e. Low: < 6 mm, Medium: 6–12 mm, and High: > 12 mm).
- **Cracked Grids Percentage Calculation:** Calculate the percentage of cracked grids within each severity group, for each zone and the entire section using **Eq. (2)**.

$$\text{Grid-based Cracking Percentage} = n_c/N \times 100\% \quad \text{Eq. (2)}$$

Where n_c is the number of grids with cracks; N is the total number of grids

2.3.10 Step 8.2: Level 3 (JPCP) Slab State Reporting

For JPCP, in Level 3, revised WOD-288 introduced the slab state reporting definition according to a modified LTPP slab state definition, which was originally proposed by Dr. Georgene Geary (Geary, 2019). Detailed definitions for different slab states (i.e., NC, L1, T1, L2, T2, SS, CC) can be found in the Phase 1 interim report. The following **Figure 5** illustrates the different states of the slab, which are mainly determined by the pattern and locations of cracks.

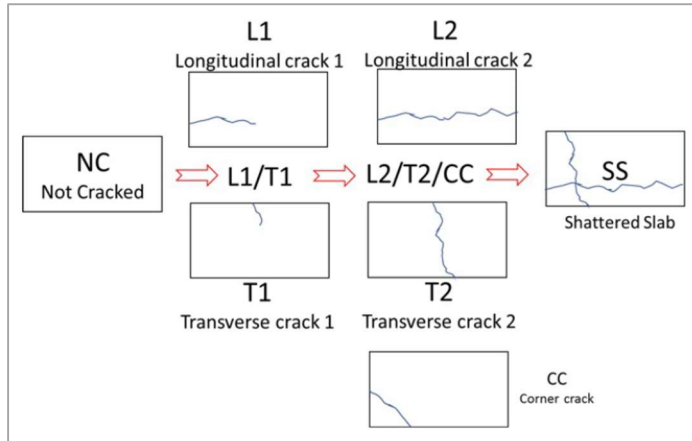


Figure 6. Slab State Definition Based on Cracking Pattern (Geary, 2019)

To implement this definition under the requirement of automation, a method is needed to classify JPCP slabs automatically. Research previously conducted by our research team has demonstrated a deep learning-based method can achieve automated JPCP slab classification (Hsieh et al., 2021). However, this method lacks interpretability and is difficult to implement practically.

Thus, we developed an innovative method based on the Crack Vector Model (CVM) and multi-dimensional cracking extent projection method to support the implementation of the newly proposed slab state definition (Yang et al., 2025). This method extracts geometric features from extent projections of crack maps at both longitudinal and transverse directions, enabling the use of tree-based models for effective slab classification. This method is robust to missing crack detection caused cracking discontinuity issues and cracking bifurcations challenges in slab classification.

Figure 7 illustrates a simplified slab classification process, derived from a trained tree-based model, using three key cracking extent features:

- **Transversal Extent (ft):** crack extent measured in the transverse direction.
- **Longitudinal-to-Transversal Extent Ratio:** ratio of longitudinal crack extent to transversal crack extent.
- **Longitudinal Extent-to-Slab Length Ratio:** ratio of the longitudinal crack extent to the total slab length.

In this study, this model is introduced to demonstrate the feasibility of implementing the new cracking slab state cracking definition for JPCP. Moving forward, the model can be further optimized by enhancing the data features and training on a larger and more diverse dataset to improve the classification accuracy.

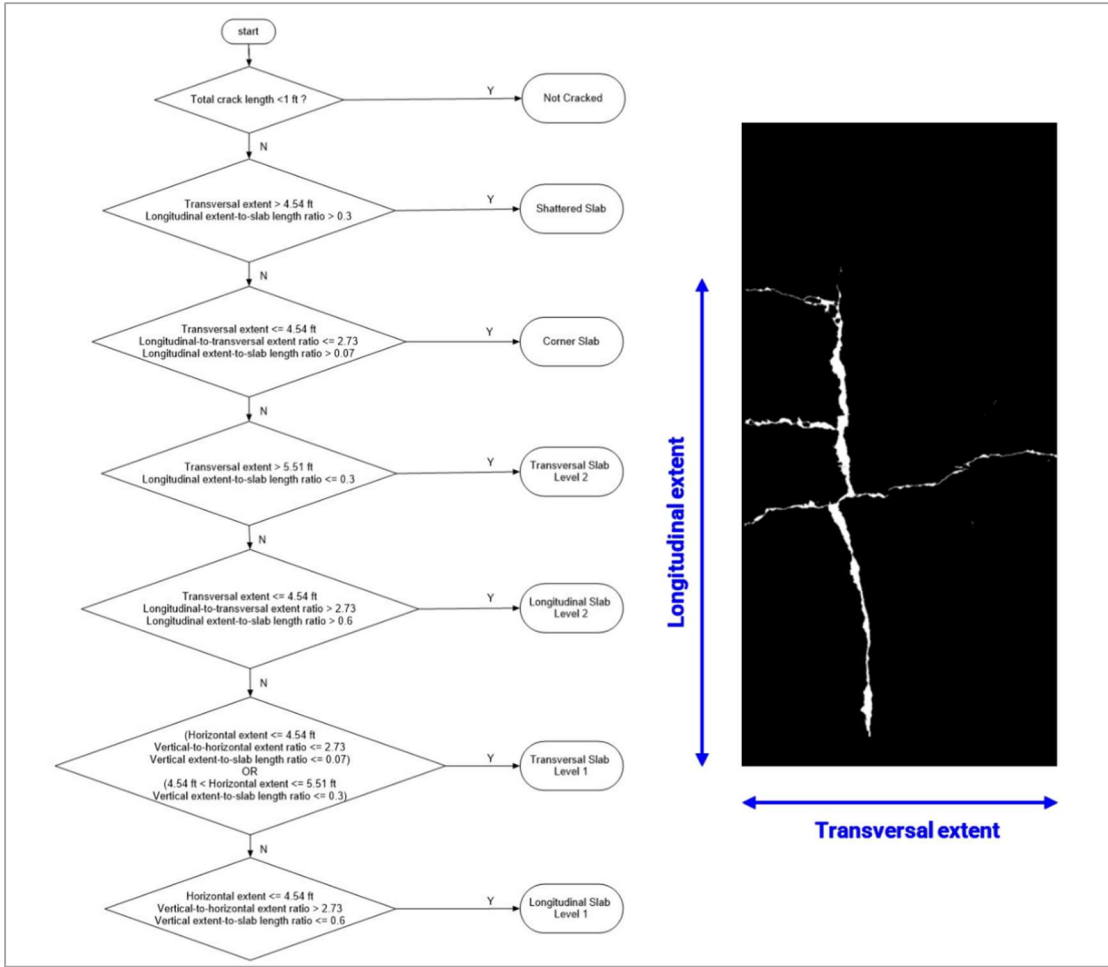


Figure 7. Flowchart for Slab Classification Process

2.4 Case Study

The feasibility of the revised WOD-288 crack definitions was assessed using real-world pavement data collected from the previous task. The case study of two asphalt pavement images with alligator cracking and transverse cracking and a JPCP image are illustrated in the report.

2.4.1 Case Study 1: Alligator Cracking Example

Case study 1 uses a pavement section with alligator cracking to illustrate the revised crack definitions are capable of extracting and measuring the alligator cracking information.

For Level 1 (Link-wise) crack information, crack features and properties were extracted from intensity and range/segmentation images and consolidated into a CVM table, as shown in **Figure 8** and **Table 6**. All the cracks within the pavement lane markings are detected and extracted.

To generate the Level 2 (Zone-wise) information, crack links were classified into categories: non-wheel-path longitudinal, transverse, wheel-path, and alligator cracks, based on criteria in **Table 5**. For this crack map, only transverse, wheel-path, and alligator cracks were identified, as shown in **Figure 9**.

For the Level 3 (Grid-based) information, the crack map is divided into grids, as shown in **Figure 10**, and the percentage of cracked grids within the 5m × 4m roadway section is calculated. Then, the crack severity for each grid is categorized by representative crack width into three pre-defined levels (low, medium, and high). The result is shown in **Table 7**, the alligator cracking example image contains only the low severity (width-based severity) cracking with an extent of 35.09%. Meanwhile, it has a 25.26% extent of wheel-path cracking with most of them in the right wheel-path.

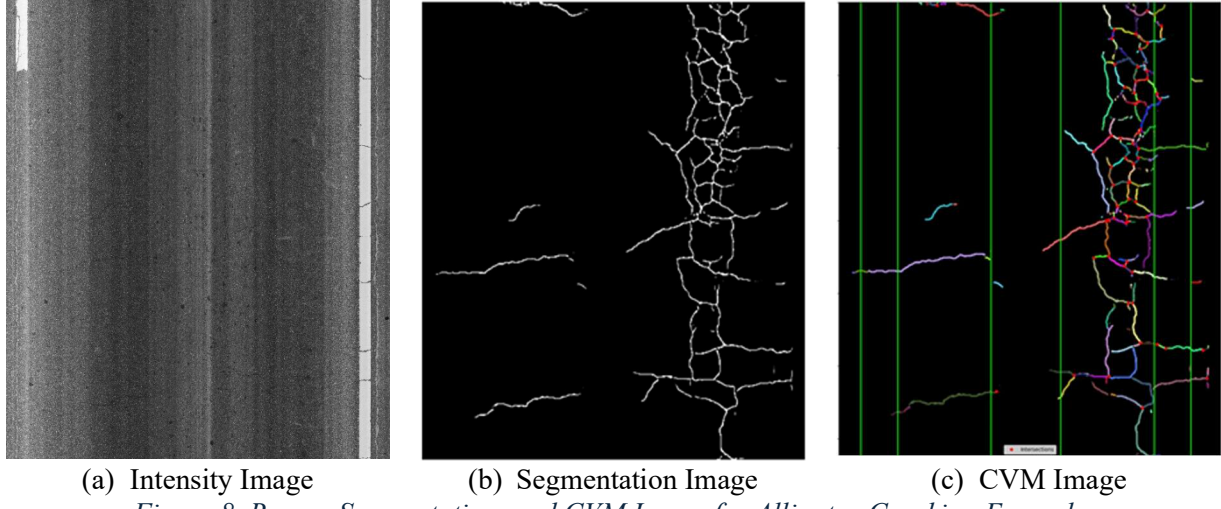


Figure 8. Range, Segmentation, and CVM Image for Alligator Cracking Example.

Table 6. Portion of CVM Table for Alligator Cracking Example.

Image ID	Zone Position (lane marking)	Link ID	Geometry	Width (mm)	Sealed Crack	Representative Width (Average) (mm)	Severity Level	Length (mm)	Orientation (deg)	Position (zone, ratio)	Alligator Crack
S1	S2	S3	S4	S5	S6	S7*	S8*	S9*	S10*	S11*	S12*
t2015-06-15_new_855_crackseg	zone1_left_px=59 zone2_left_px=159 zone3_left_px=413 zone3_right_px=603 zone4_right_px=857 zone5_right_px=957	1	[(1, 219), (1, 220), (1, 221), (1, 222), (2, 223), (3, 223), (4, 224)]	(0.0, 2.5, 2.5, 2.5, 3.5, 2.5, 0.0)	0	1.9	Low	27	59	[(2, 1.0)]	0
		2	[(1, 238), (1, 239), (2, 240), (3, 241), (4, 241), (5, 240), (6, 240)]	(0.0, 2.5, 5.0, 3.5, 3.5, 2.5, 0.0)	0	2.4	Low	28	22	[(2, 1.0)]	0
		3	[(1, 268), (2, 268), (3, 268), (4, 268), (5, 268), (6, 267), (7, 266)]	(0.0, 2.5, 2.5, 2.5, 2.5, 9.0, 0.0)	0	2.7	Low	27	18	[(2, 1.0)]	0
		...									

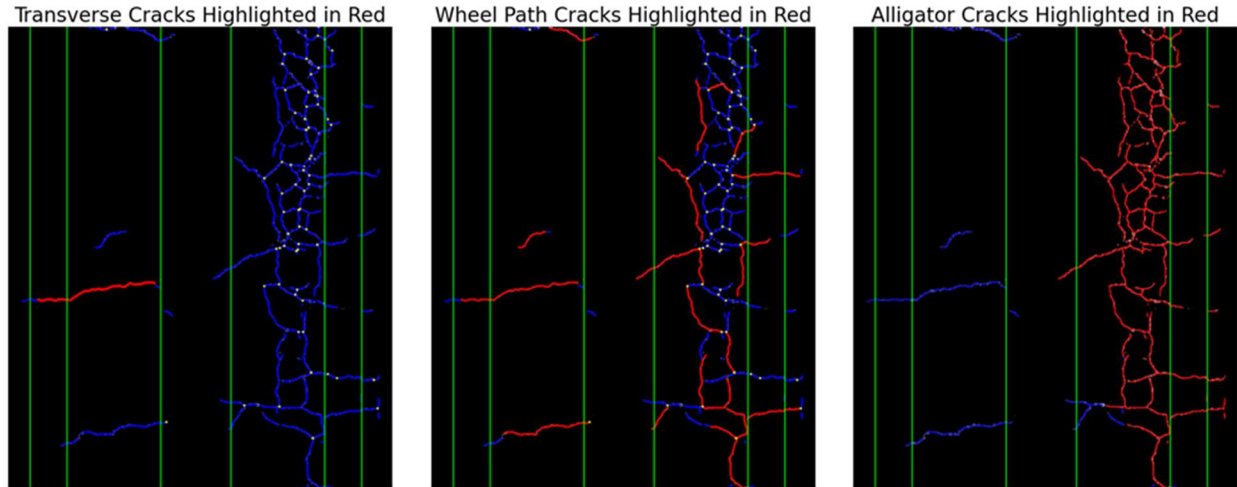


Figure 9. Level 2 Crack Classification for Alligator Cracking Example.

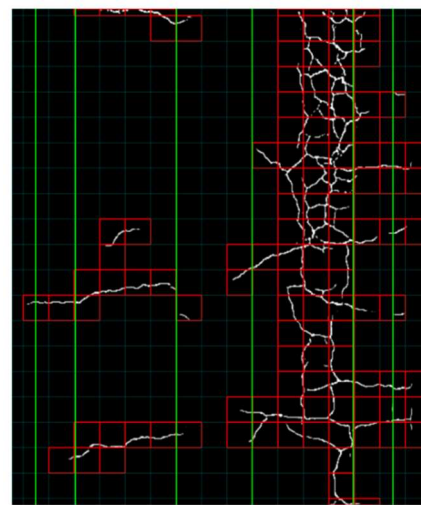


Figure 10. Overlaid Grid and Zone Boundaries for Alligator Cracking Example.

Table 7. Crack Measurement Report for Alligator Cracking Example.

Levels	Items	Item Description/Definition	Severity Level	Min. Length	Orientation	Unit	Reported Region of Interest					
							Overall	Zones				
								1	2	3	4	5
Lv. 3 (Grid-based)	3.1 Percentage of Cracks	Percentage of grids having cracks (grid size of 250 mm by 250 mm)				%	35.09%	1.05%	5.26%	2.46%	20.00%	6.32%
	3.2 Percentage of Cracks by Severity Levels	Further break down item 3.1 into three severity levels according to crack width.	L (< 6 mm) M (6–12 mm) H (> 12 mm)			%	35.09%	1.05%	5.26%	2.46%	20.00%	6.32%
	3.3 Percentage of Wheel-path Cracks	Highlight cracks within the wheel paths from all detected cracks.				%	25.26%	NA	5.26%	NA	20.00%	NA
Lv. 2 (Zone-wise)	2.1 Length of Non-wheel Path Longitudinal Cracks	Length of longitudinal cracks in zones 1, 3, and 5, defined by a crack orientation between 0° and 20° and a minimum length of 12 inches.	L M H	12 in. (end point to end point)	0° ≤ α < 20°	ft.	0	0	NA	0	NA	0
	2.2 Length of Transverse Cracks	Length of transverse cracks, which must span at least two zones with an orientation between 70° and 90°. A zone is considered spanned if the crack covers more than 50% of its width.	L		70° < α ≤ 90°	ft.	4.61	1.09	3.52	0	0	0
			M			ft.	0	0	0	0	0	0
			H			ft.	0	0	0	0	0	0
	2.3 Length of Wheel Path Cracks	Total length of cracks in zones 2 and 4, including all types (e.g., alligator cracks), must be a minimum of 12 inches.	L M H	12 in. (end point to end point)		ft.	39.02	NA	9.42	NA	29.60	NA
	2.4 Area of Alligator Cracks	The area of alligator cracking is determined by multiplying the approximate length of the affected area by the width of the wheel path zone. Items 2.2 and 2.5 are excluded from this calculation.				ft. ²	39.94	NA	0	NA	39.94	NA
	2.5 Length Sealed Cracks	Length of sealed cracks refers to any crack that has been treated with a sealant material.				ft.	NA	NA	NA	NA	NA	NA
	2.6 Length of Other Cracks	Length of other cracks includes all cracks in zones 1, 3, and 5 that are not covered in items 2.1 and 2.2.				ft.	12.32	0.50	NA	2.19	NA	9.63
Lv. 1 (Link-wise)	1 Crack Vector Model (CVM)											

Four challenges are identified during this case study:

- a) Transverse cracks are currently defined as those with an orientation between 70° and 90° and extending across at least two zones, however, because cracks can be discontinuous, certain transverse cracks may not be captured in item 2.2 (Length of Transverse Cracks) in the crack measurement report.
- b) Long (at least 12 in.) transverse and alligator cracks in wheel path zones are also categorized as wheel path cracks, this practice can result in duplicate counts.
- c) Only the wheel path zones are considered when calculating the area of alligator cracking. Yet, alligator cracking can extend outside these zones, additionally, the current methodology measures the alligator cracking impacting area by its longitudinal extent, unable to reveal the severity of cracking conditions when alligator cracks spread more extensively in the transverse direction.
- d) Cracks under 12 in. in length in zones 2 and 4 are omitted from the report.

2.4.2 Case Study 2: Transverse Cracking Example

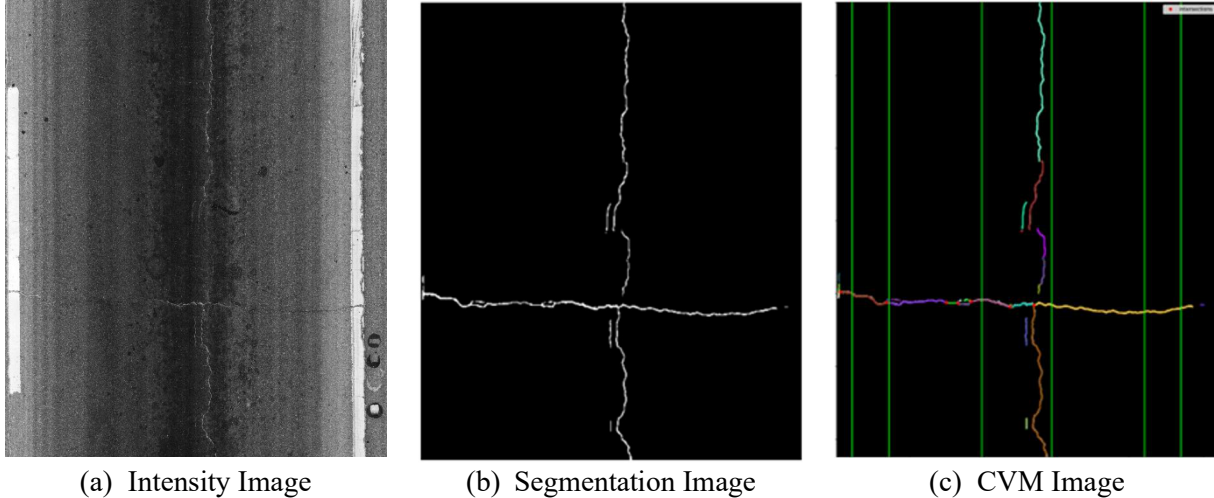
The purpose of case study 2 is to illustrate the revised crack definitions that can also support other crack types, using transverse crack in this case.

The same procedure is conducted to extract Level 1 (Link-wise) crack features and properties, as shown in **Figure 11** and **Table 8**. Level 2 (Zone-wise) information is then generated by classifying crack links into different crack types under the pre-defined criteria. Only the longitudinal, transverse, and wheel-path cracks are part of this example, as shown in **Figure 11**.

Level 3 (Grid-based) information is extracted with overlaid grids on crack maps, as shown in **Figure 13**, and the percentage of cracked grids within the 5m × 4m roadway section is calculated. Then, the crack severity for each grid is categorized. The result is shown in **Table 9**, the transverse cracking example image

is dominated by 14.02% low severity cracking with a small portion of medium severity cracking of 0.35% extent. Meanwhile, it only has a 3.15% extent of wheel-path cracking evenly distributed in both wheel-paths.

The challenges (a), (b), and (d) encountered in the case study 1 also occurred during the case study 2.



(a) Intensity Image (b) Segmentation Image (c) CVM Image
Figure 11. Range, Segmentation, and CVM Image for Transverse Cracking Example.

Table 8. CVM Table for Transverse Cracking Example.

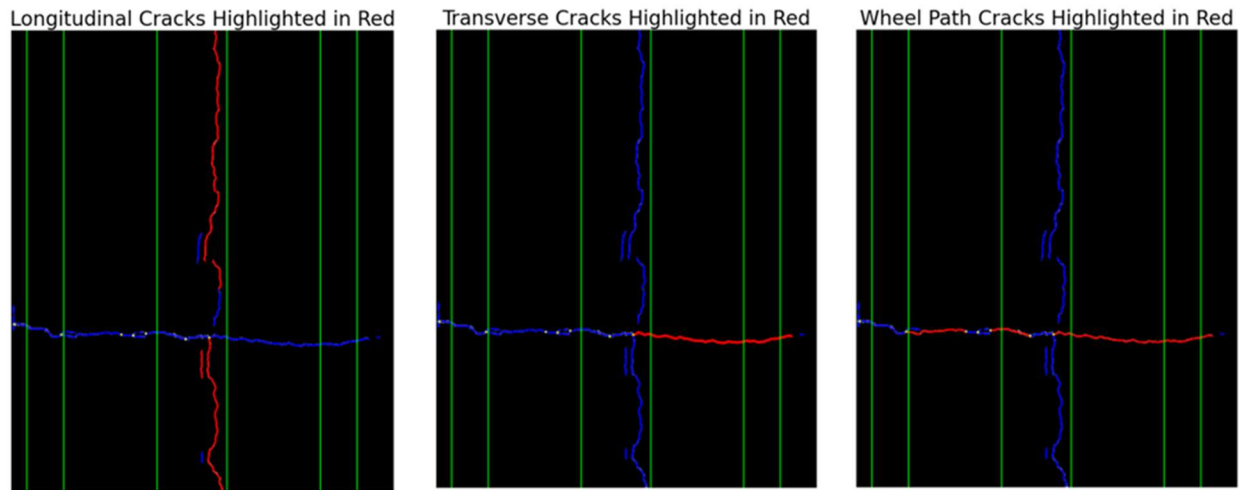


Figure 12. Level 2 Crack Classification for Transverse Cracking Example.

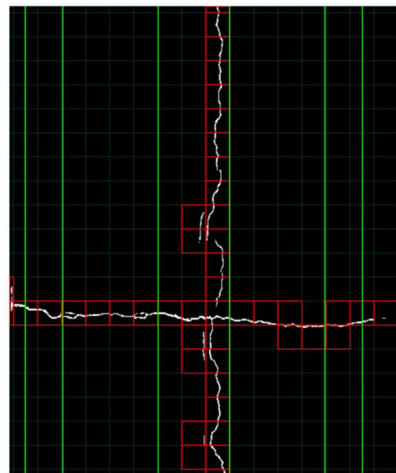


Figure 13. Overlaid Grid and Zone Boundaries for Transverse Cracking Example.

Table 9. Crack Measurement Report for Transverse Cracking Example.

Levels	Items	Item Description/Definition	Severity Level	Min. Length	Orientation	Unit	Reported Region of Interest						
							Overall		Zones				
							1	2	3	4	5		
Lv. 3 (Grid-based)	3.1 Percentage of Cracks	Percentage of grids having cracks (grid size of 250 mm by 250 mm)					%	14.37%	0.70%	1.40%	9.47%	1.75%	1.05%
	3.2 Percentage of Cracks by Severity Levels	Further break down item 3.1 into three severity levels according to crack width.					%	14.02%	0.35%	1.40%	9.47%	1.75%	1.05%
	3.3 Percentage of Wheel-path Cracks	Highlight cracks within the wheel paths from all detected cracks.					%	0%	0%	0%	0%	0%	0.00%
							%	3.15%	NA	1.40%	NA	1.75%	NA
Lv. 2 (Zone-wise)	2.1 Length of Non-wheel Path Longitudinal Cracks	Length of longitudinal cracks in zones 1, 3, and 5, defined by a crack orientation between 0° and 20° and a minimum length of 12 inches.	L ($< 6 \text{ mm}$)	12 in. (end point to end point)	$0^\circ \leq \alpha < 20^\circ$		ft.	17.42	0	NA	17.42	NA	0
							ft.	0	0	NA	0	NA	0
							ft.	0	0	NA	0	NA	0
	2.2 Length of Transverse Cracks	Length of transverse cracks, which must span at least two zones with an orientation between 70° and 90°. A zone is considered spanned if the crack covers more than 50% of its width.	M ($6\sim12 \text{ mm}$)		$70^\circ < \alpha \leq 90^\circ$		ft.	5.81	0	0	0.73	3.64	1.44
							ft.	0	0	0	0	0	0
							ft.	0	0	0	0	0	0
	2.3 Length of Wheel Path Cracks	Total length of cracks in zones 2 and 4, including all types (e.g., alligator cracks), must be a minimum of 12 inches.	H ($> 12 \text{ mm}$)	12 in. (end point to end point)			ft.	6.36	NA	2.72	NA	3.64	NA
							ft.	0	NA	0	NA	0	NA
							ft.	0	NA	0	NA	0	NA
	2.4 Area of Alligator Cracks	The area of alligator cracking is determined by multiplying the approximate length of the affected area by the width of the wheel path zone. Items 2.2 and 2.5 are excluded from this calculation.					ft. ²	0	NA	0	NA	0	NA
	2.5 Length Sealed Cracks	Length of sealed cracks refers to any crack that has been treated with a sealant material.					ft.	NA	NA	NA	NA	NA	NA
	2.6 Length of Other Cracks	Length of other cracks includes all cracks in zones 1, 3, and 5 that are not covered in items 2.1 and 2.2.					ft.	6.47	1.69	NA	4.78	NA	0
Lv. 1 (Link-wise)	1 Crack Vector Model (CVM)												

2.4.3 Case Study 3: JPCP Cracking in a 0.1-Mile Section (Slab ID #947 to #986)

Case study 3 aims to validate the feasibility of revised crack definitions for JPCP pavement, covering a 0.1-mile section consisting of 40 slabs. The slabs are numbered as slab IDs #947 to #986. Image ID varies by each slab; one slab can be in one image or in adjacent images. Table 10 shows a slab that is in adjacent images (047556 and 047557).

For Level 1, the JPCP report, as shown in Table 10, follows a similar structure to the asphalt pavement report, where nodes and links are assigned coordinates and widths. However, there are key differences:

- Crack Association with Slabs: All cracks terminate at slab joints and are linked to a specific slab. The Slab ID column (S1) associates each crack with its slab.
- Depth Measurement (S8): In addition to crack width, JPCP cracks include a depth measurement. This additional metric is intended to support future efforts in distinguishing map cracking from structural cracking.

Table 10. CVM Table for JPCP Cracking Case Study

Image ID	Slab ID	Link ID	Geometry	Width (mm)	Representative Depth (mm)	Sealed Crack	Representative Width (Average) (mm)	Length (mm)	Orientation (deg)
S1	S13	S3	S4	S5	S14	S6	S7*	S9*	S10*
047556-047557	947	1	[(0, 906), (1, 906), (2, 906)]	(0.0, 1.5, 0.0)	N/A	0	0.5	8	0
		2	[(3, 901), (3, 902), (3, 903), (3, 904)]	(0.0, 1.5, 1.5, 0.0)	N/A	0	0.8	12	90
		3	[(5, 892), (5, 891), (6, 890), (6, 889), (6, 888), (6, 887), (6, 886)]	(0.0, 2.5, 1.5, 1.5, 1.5, 0.0)	N/A	0	1.2	25	81
		4	[(10, 866), (10, 867), (10, 868)]	(0.0, 1.5, 0.0)	N/A	0	0.5	8	90
		5	[(17, 831), (17, 832)]	(0.0, 0.0)	N/A	0	0.0	4	90
		...							

For Level 2 information shown in Figure 14, all slabs are labeled as cracked or non-cracked based on their presence in the CVM table—if a slab ID appears in the CVM table, it is classified as cracked; otherwise, it is classified as non-cracked. Consequently, 21 of 40 slabs are identified as cracked in the case study section. For each cracked slab, the number of intersections is recorded. Meanwhile, cracked slabs in the section are categorized based on crack orientation:

- Longitudinal Cracks: $0^\circ \leq \text{orientation} < 20^\circ$
- Transverse Cracks: $70^\circ < \text{orientation} \leq 90^\circ$
- Other Cracks: Cracks besides the longitudinal and transverse classifications

After the crack type classification, the following metrics are computed for each crack category:

- Total Length (mm): The sum of crack link lengths for all slabs in the category.
- Weighted Average Width (mm): The average crack width, calculated by weighting each crack link width according to its length. This ensures that longer cracks contribute more significantly to the final average width than shorter cracks.

Distress Type	Description	Rating Interval/Subsection												Section Total	
		947	948	...	952	953	954	...	962	963	964	...	985	986	
Slabs with Crack	Y=1/N=0	1	0		1	1	1		0	0	1		0	0	21/40
	Intersection Count	12	None		9	17	10		None	None	0		None	None	
	Total Length (mm)	212	None		451	3,114	3,178		None	None	966		None	None	19,823
Longitudinal	Weighted Average Width (mm)	2.79	None		4.06	6.48	4.07		None	None	6.40		None	None	
	Total Length (mm)	3,648	None		3,754	3,766	3,516		None	None	0		None	None	54,302
	Weighted Average Width (mm)	5.10	None		4.96	5.82	3.88		None	None	0		None	None	
Transverse	Total Length (mm)	202	None		859	2,973	544		None	None	0		None	None	25,697
	Weighted Average Width (mm)	3.74	None		4.75	4.78	7.34		None	None	0		None	None	
Other	Total Length (mm)														
	Weighted Average Width (mm)														

Figure 14. JCP Level 2 Report Sample

For Level 3 reporting, slabs are divided into six categories (NC: Not Cracked, SS: Shattered Cracking Slab, CC: Corner Cracking Slab, T2: Transverse Cracking Slab Level 2, L2: Longitudinal Cracking Slab Level 2, T1: Transverse Cracking Slab Level 1, and L1: Longitudinal Slab Level 1) following the process described in **Figure 7**, some examples are shown in **Figure 15**. In this case study section:

- 47.5% (19/40) are Not Cracked
- 15% (6/40) are Shattered Slabs
- 32.5% (13/40) are Transversal Slab Level 2
- 5% (2/40) are Longitudinal Slab Level 1

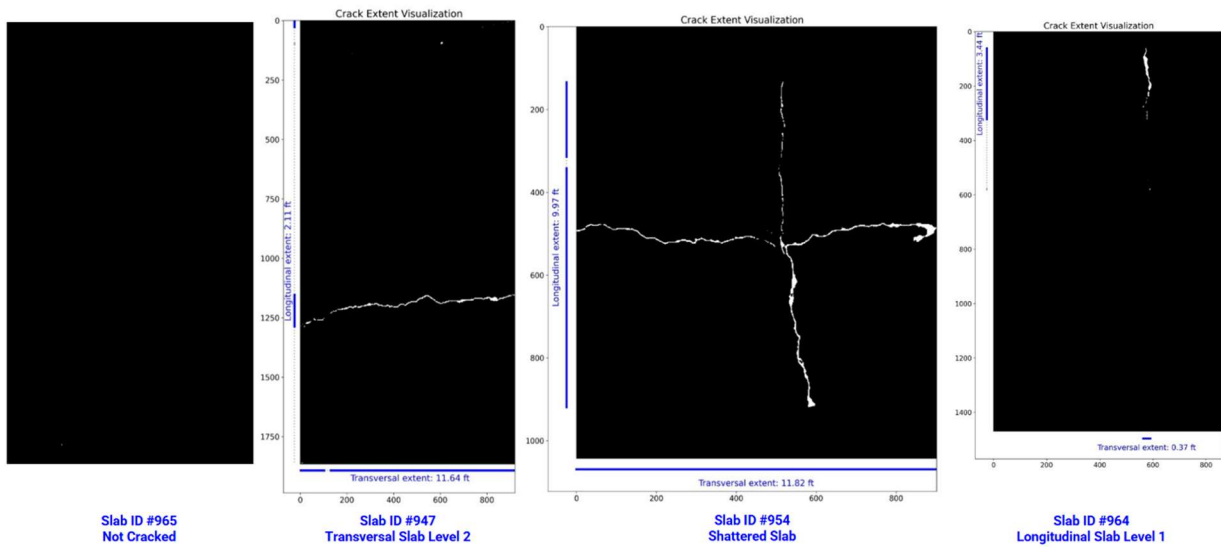


Figure 15. Sample JCP Slab Classification at Level 3

2.5 Identified Challenges

During the validation process, several key challenges were identified that impact the accuracy and usability of the revised WOD 288 Crack Definitions. Addressing these challenges is crucial to ensuring consistent application of the definitions and producing meaningful results across different pavement sections and crack types.

2.5.1 Zone-grid-displacement Issue

The size and placement setting of grids for Level 3 crack information generation might introduce displacement issues on the different pavement zones under diverse pavement conditions (for example, the narrower wheelpath in the FDOT field trip), which will cause certain grids to span multiple zones. This challenge would impact all items in the crack measurement report (example of **Table 9**). It comes from the lack of clear guidelines for handling grids that overlap multiple zones or extend beyond designated boundaries. This ambiguity complicates the measurement and classification of cracks, particularly when they span both wheel-path and non-wheel-path regions. Without standardized procedures, inconsistencies can occur in data reporting and analysis, undermining the reliability of zone-specific measurements.

2.5.2 Non-exclusive Crack Type Classification

The revised definitions lack precise and exclusive criteria for distinguishing between different crack types, potentially leading to misclassifications and double counting. This challenge would impact on the proposed Level 2 crack definition, especially the items 2.1, 2.2, and 2.3 in the crack measurement report (**Table 2**) that are based on the crack-type classification. Common issues include:

- **Misclassification between transverse cracks and wheel-path cracks:** Transverse cracks that span zones 2 and 4 may be mistakenly counted as wheel-path cracks.
- **Misclassification between long alligator cracks and wheel-path cracks:** Alligator cracks longer than 12 inches are often categorized as wheel-path cracks, double-counting one crack as two different types of cracks.
- **Misclassification between longitudinal cracks and wheel-path cracks:** Longitudinal cracks passing through zones 2 or 4 but primarily located in the other zones (1, 3, or 5) can also be incorrectly classified as wheel-path cracks and lead to double-counting issues.

These scenarios highlight the need for clearer and mutually exclusive classification criteria or a classification hierarchy to prevent the unintentional inclusion of a single crack in multiple categories, which will lead to the overestimation of the crack condition of the pavement sections. It is recommended to first identify the alligator cracking extent and exclude those areas from additional classification and to only include longitudinal and ‘other’ cracking in wheelpath cracking to reduce double counting.

2.5.3 Extent Constraints of Alligator Cracking Area Measurement

The current WOD 288 definitions focus solely on alligator cracking within the wheel-path (zones 2 and 4 in **Figure 16**), while these cracks may extend beyond the defined wheel-path zones. The current definition fails to capture the full extent of alligator cracking, as it only considers the length of the affected wheel-path zone. This issue affects Level 2 crack definition, specifically item 2.4 in the crack measurement report for the alligator crack area.

In addition, the current measurement method would record the same area measurement if the impacting lengths of two alligator cracks are identical, regardless of whether they span a small area or extend across a larger area (as shown in Figure 16). This could lead to false equivalence in alligator cracking extent measurement and result in an underestimation of pavement deterioration, particularly in cases where alligator cracks mainly deteriorate to the transverse extent. By identifying the alligator cracking extent, the degree of alligator cracking could be further stratified/defined by the density of cracking, intersections, and/or crack links, etc.

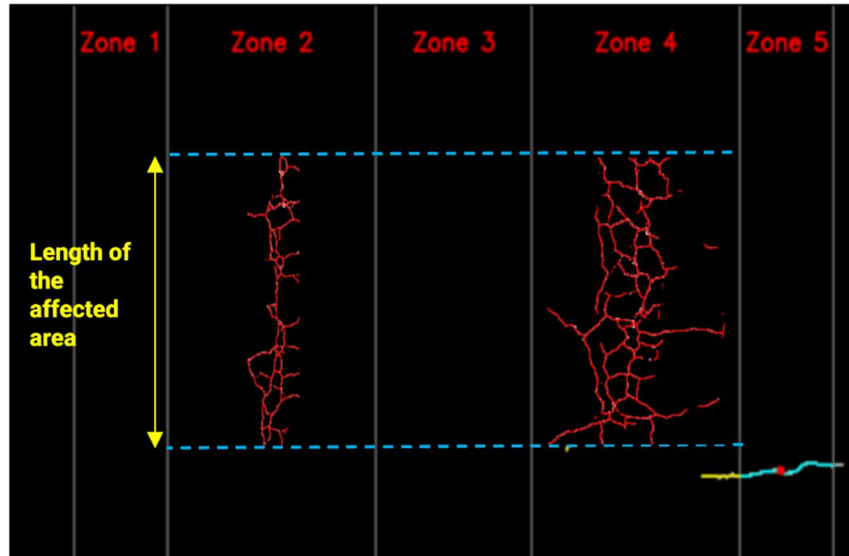


Figure 16. Illustration of Calculation of the Area of Alligator Cracking.

2.5.4 Omission of Short Non-wheelpath Cracks

A further limitation that impacts the Level 2 crack definition (item 2.6 in the crack measurement report for the length of other types of cracking) involves the exclusion of cracks under 12 inches in length within zones 1, 3, and 5, which are not reported under the revised definitions. This omission may overlook smaller cracks that indicate early signs of pavement distress. Including these shorter cracks in the reporting would enhance early detection and facilitate more effective preventive pavement maintenance.

The above challenges emphasize the need for further refinement to the revised WOD 288 definitions to improve zone-based reporting, ensure accurate crack classification, and fully capture the extent of pavement distress across all sections and crack types.

2.6 Proposed Refinement

To address the challenges identified in the validation of the revised WOD 288 Crack Definitions, several refinements are proposed to improve the accuracy, consistency, and usability of zone-based crack measurements and crack-type classifications across different pavement sections.

2.6.1 Solutions for Zone-grid-displacement Issue

To provide an immediate solution for the displacement issue, the proposed refinement recommends assigning the grid to the predominant zone that contains more than 50% of the grid area. This

recommendation also applies to grids that partially extend into Zone 1 or Zone 5 and go beyond designated lane marking boundaries, ensuring a consistent approach to handling boundary cases. Furthermore, for cracks spanning multiple zones, the wheel paths will divide the crack measurements.

To further address this issue in a fundamental way, it is recommended to identify cracking in asphalt for Level 3 in relation to zones, similar to Level 3 in JPC, using slabs instead of grids.

2.6.2 Revision for Non-exclusive Crack Type Classification

To minimize misclassifications and double counting issues, ensuring that crack types remain mutually exclusive, the revision is proposed to redefine previous "wheel path cracks" as "longitudinal cracks (wheel path)," applicable to cracks that meet the following criteria:

- Located within zones 2 or 4
- At least 12 inches in length
- Oriented between 0° and 20°
- Not classified as alligator cracks

This redefinition will reduce the potential misclassification and double counting, providing clearer distinctions between crack types.

2.6.3 Advice for Extent Constraints of Alligator Cracking Area Measurement

To improve the accuracy of alligator cracking measurements, it is recommended that measurements of the alligator cracking include both wheel-path and non-wheel-path zones, rather than limiting the assessment to the wheel path alone.

Besides the expansion of the measurement area. The wheel path length-based measurement method is also proposed to be modified using the Grid-based approach. Adopting a Grid-based approach will enable a more precise calculation of the area affected by alligator cracking, offering a more comprehensive evaluation of alligator cracking extent on the pavement surface.

2.6.4 Recommendation for Omission of Short Non-wheelpath Cracks

The current definitions exclude cracks shorter than 12 inches within zones 1, 3, and 5 from the "other cracks" category, potentially missing early indicators of pavement distress. To address this, it is recommended to include these shorter cracks, offering a more comprehensive representation of pavement conditions and aiding in preventive maintenance efforts.

These proposed refinements aim to ensure that the revised crack definitions deliver accurate, actionable insights across multiple reporting levels, from zone-based measurements to specific crack-type classifications.

3 Sensitivity Analysis

During the preliminary experiment and the process of feasibility study of the proposed revised crack definition, the research team identified the variance of extracted crack information using different parameter settings in the crack information extraction algorithm, this type of sensitivity would impact the consistency of crack measurement and analysis. So, this chapter performs the sensitivity study of the most important

parameters: 1) grid size and position settings for Level 3 crack information extraction, 2) crack width thresholding setting for crack severity classification, and 3) crack orientation thresholding setting for crack type classification. This section analyzes their impact on the output results and makes preliminary recommendations for the appropriate value ranges for these settings.

3.1 Sensitivity Study of Grid Settings (Size and Location)

The impact of grid settings of size and position have been noticed during the algorithm development; to better understand their impact, a sensitivity analysis was conducted on 120 asphalt pavement images representing four crack types: longitudinal, transverse, block cracking, and alligator cracks. The analysis examined grid sizes ranging from 24 mm (1 in.) to 508 mm (20 in.) to observe crack percentages variance with changes in grid size. Different grid positions were evaluated on each grid size by shifting the grid to the right side of the image in increments from $0\times$ to $0.9\times$ of the grid size with a step of $0.1\times$ grid size. To avoid the impact of the partial grids on the image edges and ensure consistency in calculations, only grids with at least 50% original size were included in the crack percentage analysis.

3.1.1 Grid Size Analysis

The grid-based crack percentage increased significantly as the grid size increased, the example crack map in Figure 17 shows such an increment trend and the crack percentage is expected to increase to 100% ultimately:

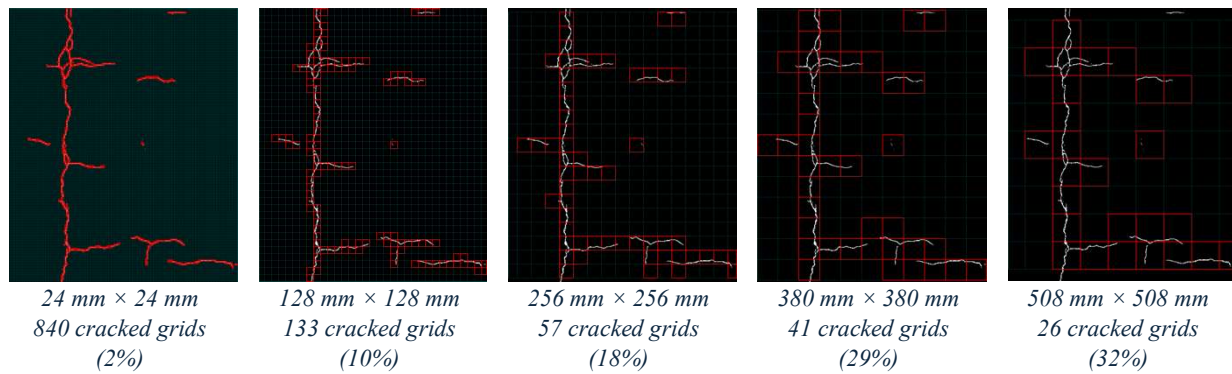


Figure 17. Illustration of Crack Percentage Variations Using Different Grid Sizes.

3.1.2 Shifting Position Analysis

The grid size of $256 \text{ mm} \times 256 \text{ mm}$ is chosen since it can provide detailed crack information while avoiding being too sensitive to the potential crack map variances caused by data quality or data processing issues. Under this grid size setting, the crack percentage fluctuated in a relatively small window (around 3%) as the grid shifted, as Figure 18 shows below:

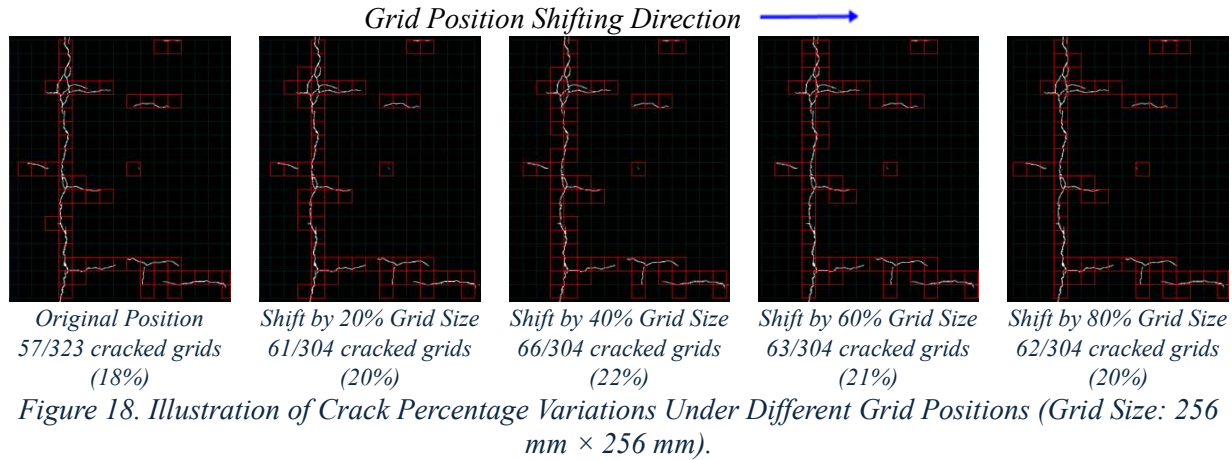


Figure 18. Illustration of Crack Percentage Variations Under Different Grid Positions (Grid Size: 256 mm × 256 mm).

The same validation procedure was implemented across 120 asphalt pavement images representing all crack types, and similar patterns were observed. The research team acknowledges the need for the grid-based output percentage value to align with the engineering instinct. Yet, the approach to selecting the optimal grid size to fulfill such a need is lacking, which requires further discussion and study. Although it is recognized that having a grid size that is an even multiple of the main defined zones (2, 3 and 4) is desirable.

3.2 Sensitivity Study of Crack Width Thresholds for Crack Severity Classification

The crack width threshold selection is important for crack severity classification. So, crack width distributions are analyzed across crack types, including longitudinal, transverse, and alligator cracking, to assess the statistical representation of crack width. The average width is used in the study as it is recommended in WOD-288.

The analysis using the same 120 asphalt pavement images mentioned above shows the majority of crack lengths fall within a width range of 2–6 mm, with widths of 3–4 mm accounting for the most significant proportion across all types, as illustrated in **Figure 19**. For different crack types, the width distribution shows different characteristics: longitudinal and transverse cracks have narrow distributions with limited variation, while block cracking and alligator cracks have wider distributions with a longer tail on the right, indicating the potential of propagating to wider cracks.

Though the distribution of crack width among different crack types is consistent and distinct, it is still impractical to select thresholds for severity classification that are robust enough for the potential width variance issues caused by data quality or data processing. So, the representative width of the crack is recommended for crack severity instead of level-based representation.

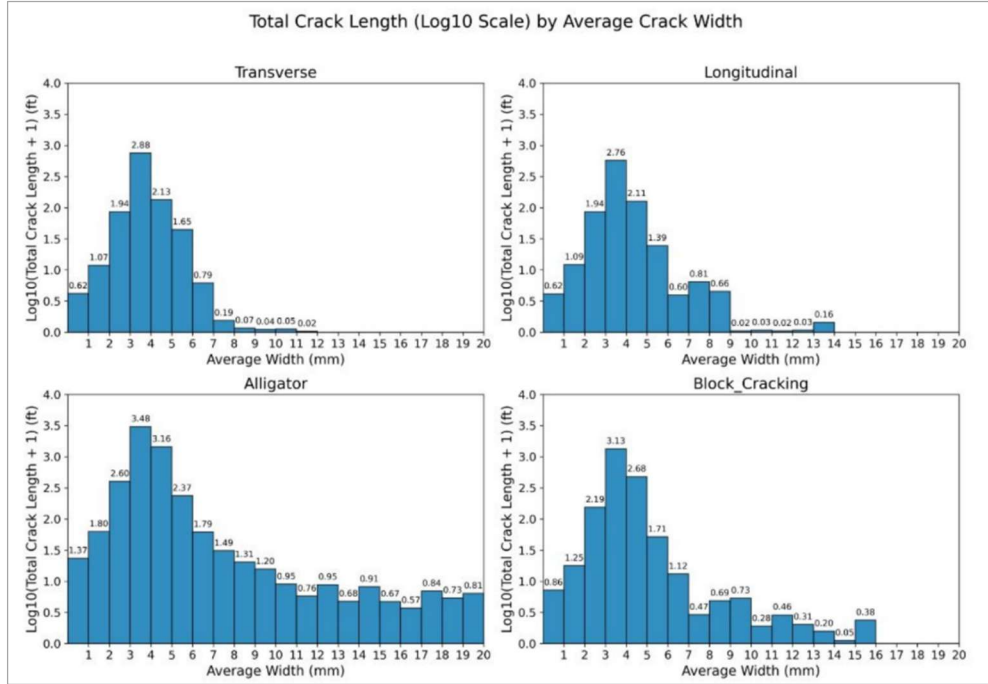


Figure 19. Average Crack Width Distribution by Total Crack Length (Log Scaled).

3.3 Sensitivity Study of Crack Orientation Thresholds for Crack-type Classification

To validate the crack orientation thresholds defined in the revised WOD-288 and confirm their effectiveness in distinguishing between different crack types. Orientations for different crack types are assessed using the same 120 asphalt crack maps as previous studies. The current thresholds in revised WOD-288 are: 1) longitudinal cracks: $0^\circ\text{--}20^\circ$, and 2) transverse cracks: $70^\circ\text{--}90^\circ$.

The result from **Figure 20** shows that the thresholds effectively categorized crack types based on orientation:

- Longitudinal cracks predominantly fall between $0^\circ\text{--}20^\circ$.
- Transverse cracks are concentrated in the range of $70^\circ\text{--}90^\circ$.
- Alligator and block-cracking consist of longitudinal cracks more than transverse cracks.

It is important to note that the categories of cracking images analyzed in **Figure 20** are classified based on the predominant cracks in the selected images. While transverse cracking images may include longitudinal cracks, and vice versa, the selection of images is based on the dominant crack type. Examples of longitudinal cracking images are provided in the Appendix, **Figure 35-39**.

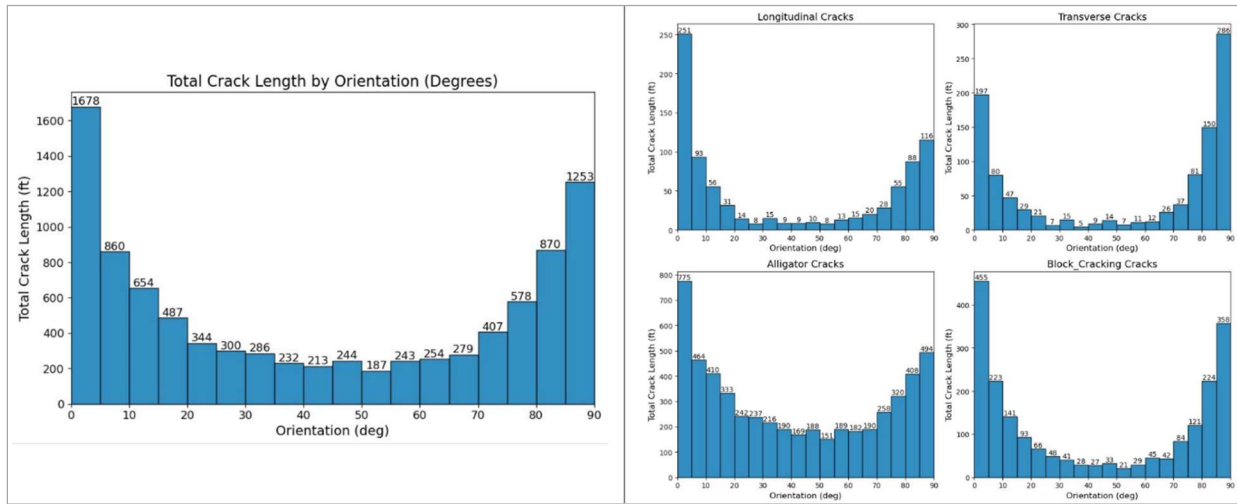


Figure 20. Crack Orientation Distribution by Crack Types.

4 HPMS Reporting Using Revised WOD-288

Reporting HPMS cracking percentage for asphalt pavement using revised crack definitions is conducted in this section to examine the utility of the proposed cracking definition.

4.1 HPMS Definition of Cracking Percentage Report

HPMS cracking for asphalt pavements is defined as: “cracking percent is the percentage of the total area exhibiting visible fatigue type cracking for all severity levels in the wheelpath in each section” (FHWA, 2016). According to the definition, the HPMS Crack percentage will be calculated using Eq. 3):

$$HPMS\ Crack\ \% = \frac{Affected\ Area\ In\ Zones\ 2\ and\ 4}{Total\ Area\ of\ Region} \times 100\% \quad \text{Eq. 3}$$

Where “**Affected Area in Zones 2 and 4**” refers to the aggregate area impacted by alligator cracks throughout the pavement section in Zones 2 and 4; “**Total Area of Region**” refers to the full lane area along the considered length. This would include the width of the lane multiplied by the total length under consideration.

The research team recognized that the longitudinal cracking was not considered for HPMS according to the old HPMS field manual (FHWA, 2016). While in November 2020, errata to the HPMS Field Manual, it is clarified that it is supposed to include longitudinal cracks. However, the definition remains unclear to execute, and we will further explore and discuss it with SHAs during the next tasks.

Statement captured from 2020 HPMS field manual errata: For Asphalt pavements (Item 49 codes '2', '6', '7', and '8'), Cracking Percent is the percentage of the total area exhibiting visible fatigue type cracking (**both longitudinal and/or pattern**) for all severity levels in the wheelpath in each section (see Figure 4.78 for an illustration of these cracking scenarios).

4.2 Methodology

The method developed for HPMS reporting using the revised crack definition is a three-step image-wise method; the HPMS crack percentage will be calculated for each pavement image and then aggregated into section-wise, such as in 0.1-mile sections.

- **Step 1: Alligator/fatigue Crack Detection:** The first step is detecting the alligator cracks within the segmentation images. The CVM processes the crack maps and identifies intersection points, listed as coordinates, and determines if they are alligator cracking by creating a predefined buffer of ~1.31 feet and checking the region according to the following key criteria:
 - 1) **Max Link Length:** The immediate crack link being checked must not exceed 9.58 feet in length. A branch is defined as a set of consecutive crack links that includes the length of links until an intersection or the end of the crack.
 - 2) **Density Threshold:** There must be at least 5 other intersections within the buffer.
 - 3) **Branch Count:** There must be at least 10 branches within the buffer. A branch includes the length of the crack until an intersection or the end of the crack.
 - 4) **Average Link Length:** The average length of crack links within the buffer must be below 2.62 feet, differentiating large structural cracks from tight, interconnected alligator-type cracking.

The example identification of alligator cracks within a segmentation image is shown in **Figure 21**. Alligator cracks tend to fall within the wheelpath zones: Zone 2 and Zone 4.

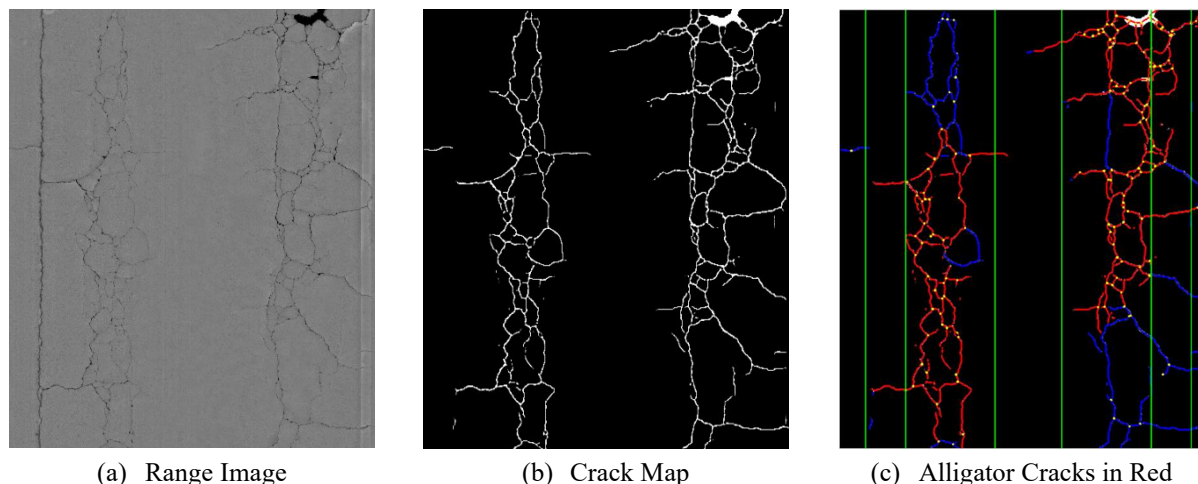


Figure 21. Illustration of Alligator Crack Detection and Classification Results.

- **Step 2: Computation of Area of Alligator Cracks:** Once all alligator cracks are located and defined, the total area of alligator cracks within Zones 2 and 4 is calculated by finding the length of affected areas within Zones 2 and 4 and multiplying by the width of Zones 2 and 4.
- **Step 3: Crack Condition Classification:** Classify the crack condition according to the criteria listed in **Table 11**.

Table 11. HPMS Cracking Conditions

Cracking Condition	HPMS Crack %
Good	<5
Fair	5-20
Poor	>20

4.3 Case Study

The following figures illustrate several instances of asphalt with differing distinctions. **Figure 22 (a)(b)** depicts asphalt with a poor HPMS crack percentage, **Figure 22 (c)(d)** depicts asphalt with a fair HPMS crack percentage, and **Figure 22 (e)(f)** depicts asphalt with a good HPMS crack percentage, based on the percentages used in HPMS.

The research team recognizes that HPMS is for a 0.1-mile section and the images are for illustration purposes only. In addition, we are also using a definition of alligator/fatigue cracking as described in **Section 4.2**, since alligator/fatigue cracking is not clearly defined in the HPMS field manual, although the Nov 2020 errata only denotes “fatigue type cracking (both longitudinal and/or pattern).” We have also noted this in the last paragraph of **Section 4.1**.

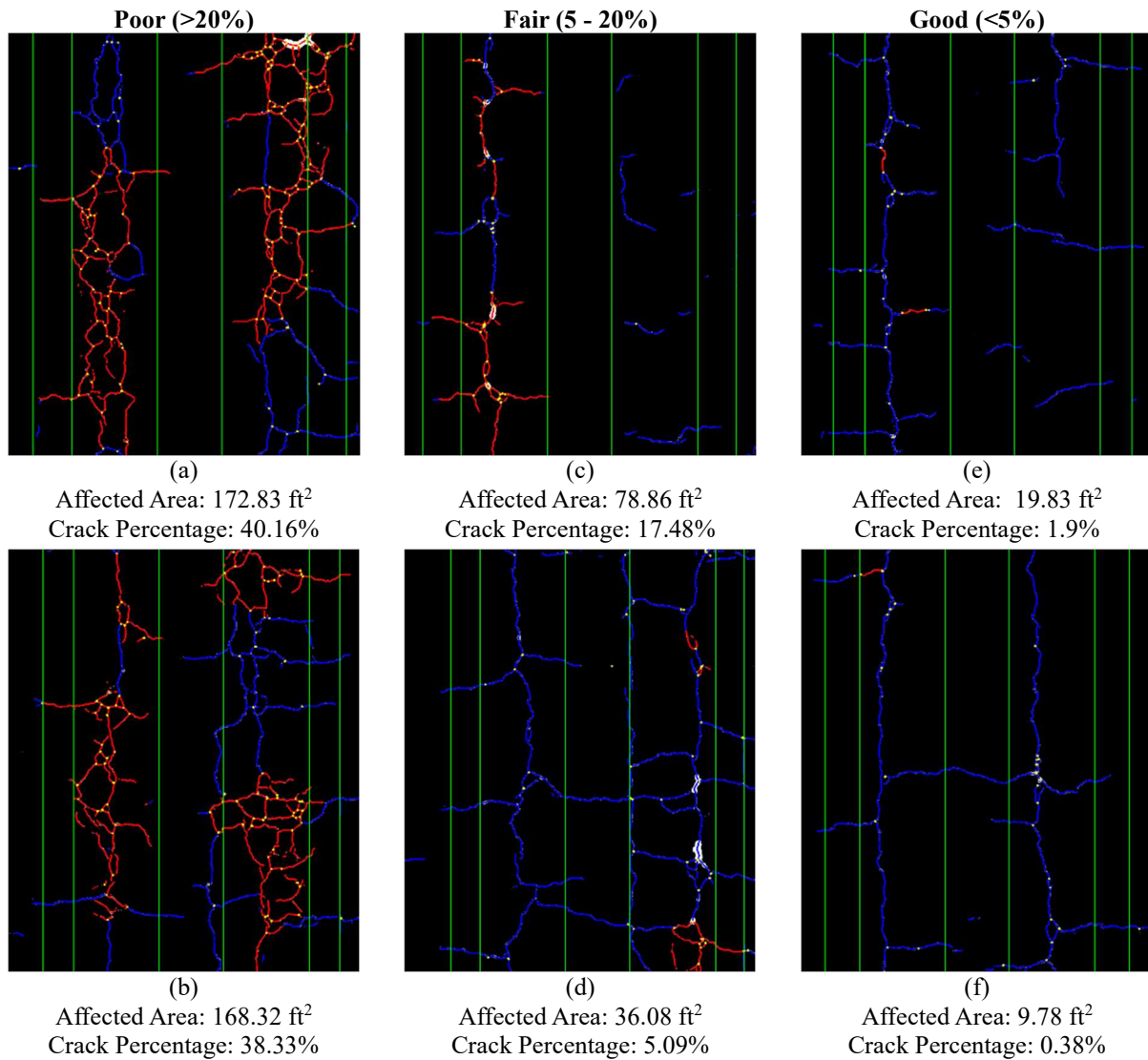


Figure 22. *HPMS Crack Images with Poor, Fair, and Good Designation*

5 Validation of Proposed Cracking Data Quality Assessment Method

This section introduces the methodology and examples from field collection data gathered in collaboration with FDOT during December 2024. The validation analysis implements two evaluation strategies previously proposed in the Task 7 report: a) end-to-end evaluation and b) decomposed evaluation.

Specifically, the validation utilizes four different ground reference methods, two for each type of strategy:

- 1) Manual surface crack mapping collected on engineering sheets using traditional field survey methods serves as the ground reference for end-to-end HPMS reporting comparison.
- 2) Manual crack augmentation on the pavement surface serves as the ground reference for end-to-end crack map detection comparison.
- 3) Scanning of ground reference boards is used for sensor quality evaluation under the decomposed strategy.
- 4) Inter-rater crack annotation is used for evaluating the accuracy of the decomposed component: the crack detection algorithm.

5.1 End-to-end Methods Validation

The end-to-end methods aim to provide ways for straightforwardly evaluating the data quality utilizing agencies' currently possessed or accessible data like HPMS reporting and crack maps, so the agencies could also conduct such data quality assessments without decomposing the data processing procedure that needs additional technical support.

5.1.1 Methodology

5.1.1.1 Two Proposed End-to-end Ground Reference Methods

The two proposed end-to-end strategies aim to establish ground references for real-world cracks and compare them with vendor-measured cracks using revised WOD-288 to assess the cracking data quality.

- **Method 1 – Manual surface crack mapping (on engineering sheet):**

This method was proposed in Phase 1 (refer to the Phase 1 Interim Report, Chapter 3.3), which was called the field-based method. This method involves experienced engineers manually drawing cracks on paper on-site to create a ground reference, which is used to evaluate whether the vendor can accurately report crack distress in accordance with the revised WOD-288. **Figure 23** presents an example of a scanned drawing of a crack map on the engineering sheet. Then the field survey expert would generate the HPMS reporting of the crack percentage accordingly.

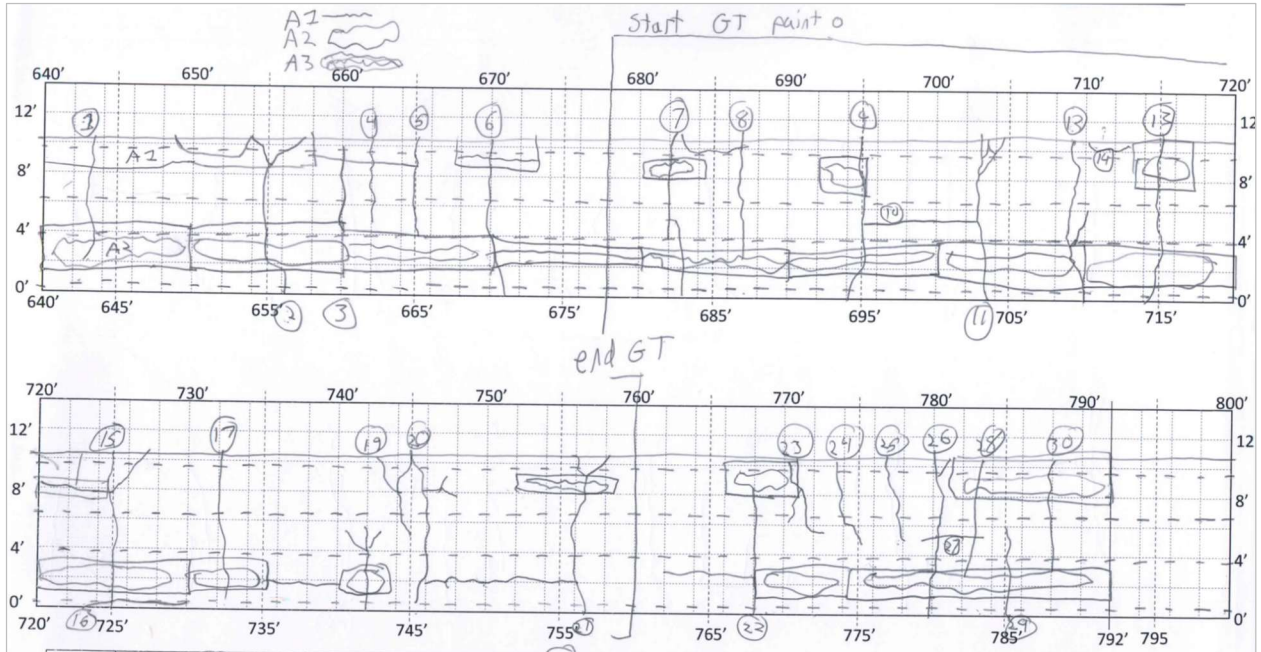


Figure 23. Sample Manual Crack Mapping on Engineering Sheets (Severe cracking condition data collected in December 2024 on a Boat Ramp Road in Gainesville, Florida).

- **Method 2 – Manual crack augmentation (on pavement surface):**

This method involves marking cracks directly on the pavement surface. High-quality images taken by drones or cameras and intensity images from testing sensors are used as references for manual annotation to create ground reference crack maps. The goal, like Method 1, is to generate a ground reference to assess the vendor's ability to accurately report crack distress according to the revised WOD-288 (e.g., crack maps). **Figure 24** shows the data involved in this method: the range, intensity images, and detected crack maps from the testing system are as shown in (a) – (c), the top-down drone images shown in (d) are used for reference together with intensity images to annotate the manual augmentation to generate manual annotations like red pixels shown in (e), and further, manual crack map annotations like (f) to serve as the ground reference for this method to conduct the cracking data quality assessment.

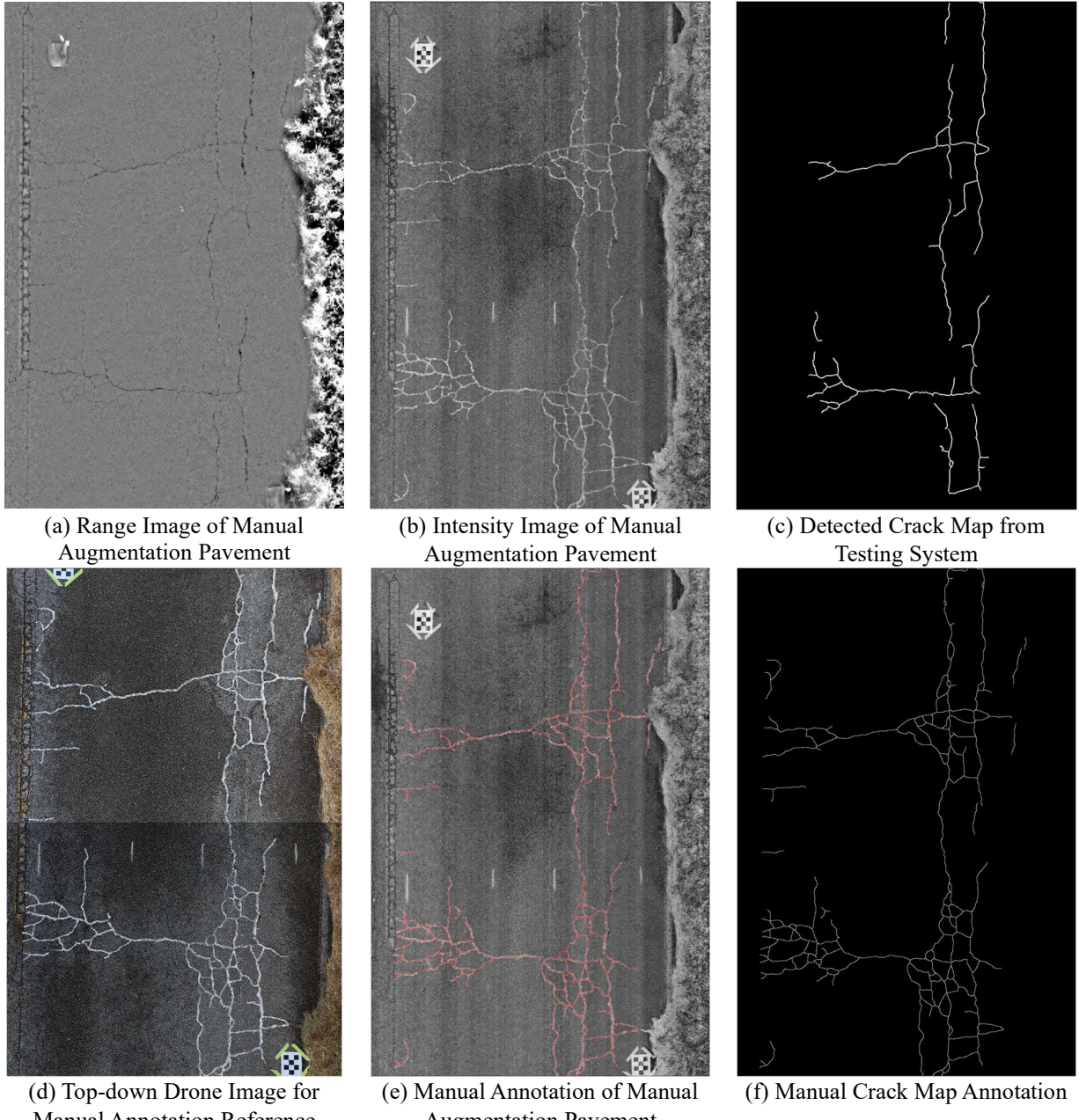


Figure 24. Illustration of Ground Reference Procedure Using Manual Crack Augmentation.

5.1.1.2 Validation Methods

Using the ground references from the two above methods, the validation of the proposed crack data quality assessment is performed through the following two methods: crack map comparison and HPMS crack percentage reporting comparison. The reason for proposing two methods is that the crack map comparison could provide detailed information for data quality assessment, yet it is unsuitable for the traditional manual crack maps on engineering sheets, which require the HPMS cracking reporting comparison to provide the data quality assessment.

Crack map comparison includes the visual assessment and Enhanced Hausdorff Distance (EHD) measurement:

- **Visual Assessment:** Qualitative comparison of crack patterns, locations, and continuity between ground reference methods and testing system outputs
- **Enhanced Hausdorff Distance (EHD) Measurement:** Quantitative metric to evaluate spatial accuracy of crack detection by measuring the EHD scores between crack maps from ground references and testing systems. Note that the crack maps on the engineering sheets are not feasible for this measurement.

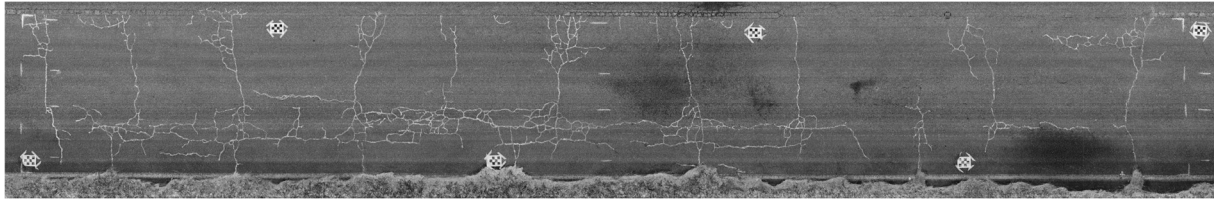
HPMS cracking percentage reporting comparison would need to generate the HPMS reporting from crack maps of the testing roadway sections from each method and compare the crack percentage.

The ground references generated under two methods and the crack results (including crack maps and HPMS crack percentage reporting) are compared using the following strategies to assess the cracking data quality of the testing systems.

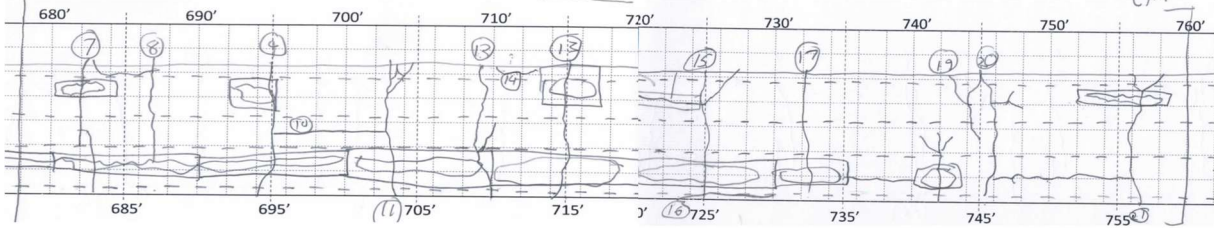
- **Ground Reference from Engineering Sheet vs. Ground Reference from Crack Augmentation:** Comparative analysis of the two ground reference methods to establish reliability benchmarks.
- **Ground Reference from Engineering Sheet vs. Data from Testing System:** Evaluation of traditional field survey methods against the testing system, assessing whether the cracking data quality from the testing systems could support agencies' utility needs.
- **Ground Reference from Crack Augmentation vs. Data from Testing System:** Assessment of manual augmentation approach against the testing system, with a focus on the cracking data quality captured by the testing systems.

5.1.2 Case Study and Results

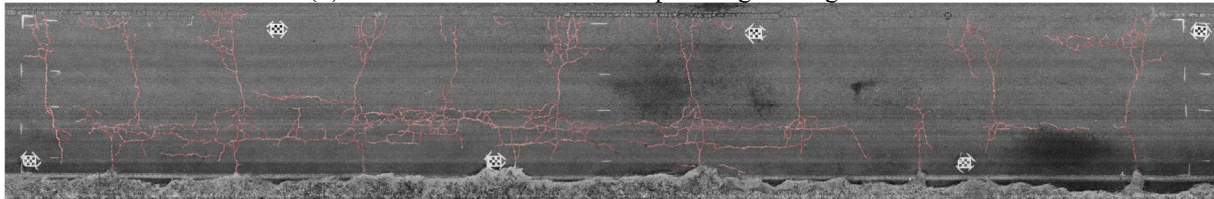
The validation of the end-to-end cracking data quality assessment methods is conducted through the case study using the data collected from the FDOT field trip in December 2024. The testing system used is the FDOT in-house LCMS-2 system, which could provide the intensity, range images, and system-detected crack information for crack map generation. The testing site is a 0.3-mile dense-graded asphalt section with ground referencing methods of a) cracking survey using engineering sheets on the whole section and b) crack augmentation using white paint on a 25-m section. **Figure 25 (a)** shows the intensity image of the crack augmentation section, **Figure 25 (b)** illustrates the corresponding crack maps on engineering sheets, **Figure 25 (c)**, is the manual annotation of the augmented crack, **Figure 25 (d)** is the binary format of the annotated crack map, and **Figure 25 (e)** contains the crack map generated by the testing system.



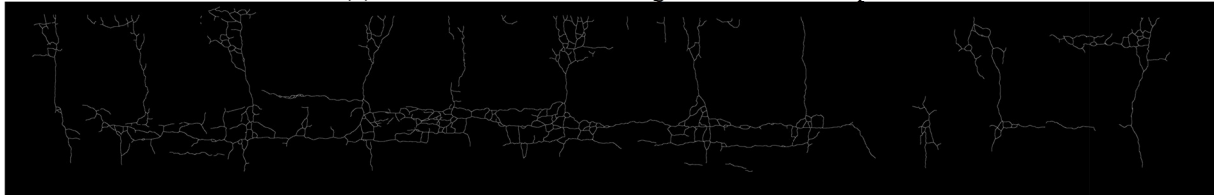
(a) Crack Augmentation in White Paint.



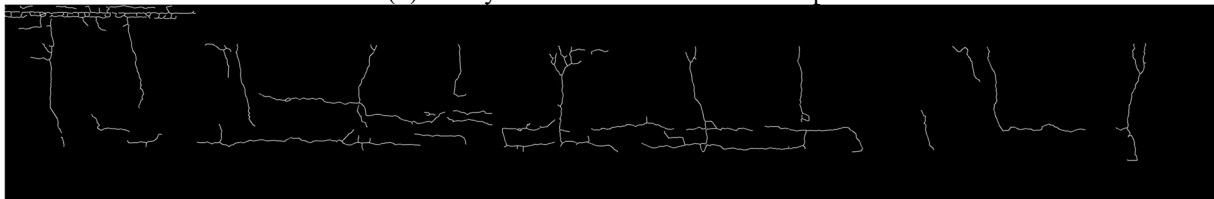
(b) Ground Reference Crack Map on Engineering Sheet.



(c) Manual Annotation of Augmented Crack Map.



(d) Binary Ground Reference Crack Map.



(e) Crack Maps from Testing Systems.

Figure 25. Case Study Section with Different Types of Crack Maps

5.1.2.1 Crack Map Comparison

- **Visual Assessment**

The visual comparison between ground references from the engineering sheet in **Figure 25 (b)** and from crack augmentation in **Figure 25 (c)** and **Figure 25 (d)** shows that the proposed crack augmentation ground reference method could achieve a similar or better level than the traditional manual survey method using engineering sheets and, hence, is able to provide supplemental crack information. It is worth noting that the results of the engineering sheet were surveyed after the crack augmentation was implemented, which might improve the detail level of the survey,

The comparison between the ground reference from the engineering sheet in **Figure 25 (b)** and the crack maps from the testing system in **Figure 25 (e)** shows that the crack maps generated from the testing system are similar to the surveyed crack maps on engineering sheets in a qualitative manner.

The comparison between the ground reference from crack augmentation in **Figure 25 (a)** and **Figure 25 (c)** and the crack maps from the testing system in **Figure 25 (e)** provides detailed information on the crack detection difference between the testing system and ground reference, which majorly happens on the short and thin cracks that serve as links within the alligator cracks.

- **Enhanced Hausdorff Distance (EHD) Measurement**

The Enhanced Hausdorff Distance (EHD) score evaluates the performance of the crack detection algorithm by comparing the crack map from the testing system to the crack augmentation ground reference, as shown in **Figure 26**. Developed by Tsai and Chatterjee (2017), EHD measures alignment between detected and actual cracks, addressing positional differences and resolution issues.

The EHD score ranges from 0 to 100 and quantifies the alignment between detected and actual crack maps, where 0 indicates a complete mismatch, and 100 represents a perfect match, with performance categorized as good above 70, moderate between 30 and 70, and poor below 30. The metric includes two penalties: the False Positive (FP) Penalty, which measures the proportion of erroneous crack pixels (ranging from 0 to 1, with lower values being better), and the False Negative (FN) Penalty, which assesses the proportion of missed actual crack pixels (also 0 to 1, with lower values being better).

The EHD results of **Figure 26** are:

- Performance Score: 34.45
- FP Penalty (False Positive Penalty): 0.32
- FN Penalty (False Negative Penalty): 0.66

The performance score of 34.45 indicates a moderate level of alignment between the detected crack map and the ground reference. The relatively high false positive penalty of 0.32 is caused by the cracks out of the lane markings that are detected by the testing system, which is acceptable as these cracks will not impact further cracking analysis and reporting. On the other hand, the false negative penalty of 0.66 indicates that a notable portion of actual crack pixels in the ground reference is missed, which aligns well with the conclusion of the testing system's discrepancy in detecting short and fine cracks from visual comparison results.

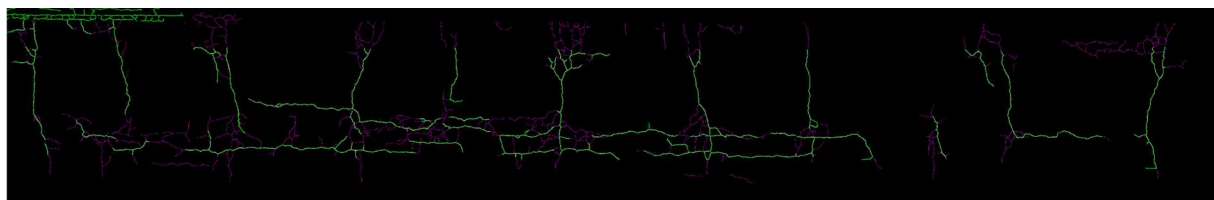


Figure 26. Crack Map Comparison Between Crack Augmentation Ground Reference (Red) and Testing System (Green).

5.1.2.2 HPMS Cracking Percentage Reporting Comparison

This section compares the HPMS cracking percentage data derived from different methods: the Engineering Sheet Ground Reference, the Crack Augmentation Ground Reference, and the testing system. Two specific analyses are presented: a comparison across the testing site augmentation section of three types of data and an evaluation over a 0.3-mile session between the engineering sheet ground reference and testing system data. The HPMS cracking percentage is calculated based on the total area of cracks within the wheel paths (defined as 39 inches wide to align with the narrow lane width of the testing section) divided by the total area of the section, consistent with HPMS guidelines.

- **Comparison Across Augmentation Section (25-m length)**

Table 12 provides a preliminary comparison of HPMS cracking percentages in the augmentation testing section using data from the Engineering Sheet Ground Reference, Crack Augmentation Ground Reference, and the testing system.

The testing system reports an extremely low cracking percentage of 0.04%, suggesting minimal alligator crack existence, aligning well with the crack detection results of the testing systems, which detect majorly the longitudinal and transverse cracks. In contrast, the Engineering Sheet Ground Reference estimates a significantly higher value of approximately 40%. The Crack Augmentation Ground Reference, with a cracking percentage of 15.42%, falls between these two, largely due to the difference in alligator cracking classification results between the proposed crack definition methods (as shown in **Figure 27**, the cracks in red are alligator crack classification results according to the proposed definitions) and the traditional survey methods (as shown in **Figure 25 (b)**, the human-drawn bounding boxes represent the alligator crack area).

Table 12. HPMS Cracking Percentage on Crack Augmentation Testing Section.

	Testing System	Engineering Sheet Ground Reference	Crack Augmentation Ground Reference
HPMS Crack %	0.04	~40	15.42

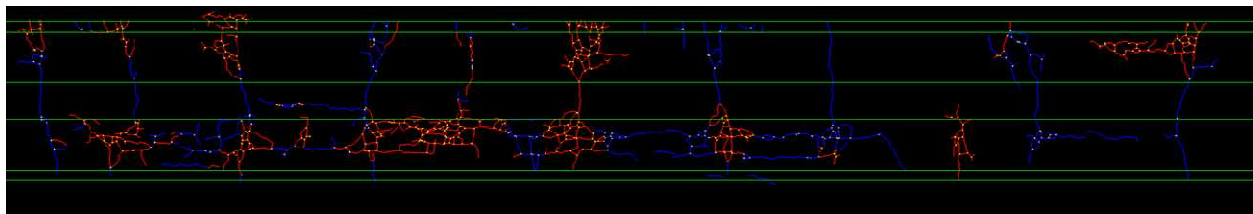


Figure 27. Alligator Crack Classification Restuls on Augmentation Section Using Proposed Crack Definitions.

- **Comparison Across the Whole Test Section (0.3-mile length)**

Table 13 and **Table 14** present detailed HPMS cracking percentages for a 0.3-mile session, divided into ten 0.03-mile subsections, using data from the Engineering Sheet Ground Reference and the LCMS testing system, respectively.

The comparison between the Engineering Sheet Ground Reference and the testing system over the 0.3-mile session reveals stark differences. The Engineering Sheet Ground Reference reports a total cracking percentage of 45%, significantly higher than the testing system's 1.81%. This discrepancy aligns with the variation of crack detection between the testing system with the crack augmentation ground reference and the differences between the alligator cracking classification results between the survey and proposed definitions.

Table 13. HPMS Cracking Percentage in 0.03 Mile Sections Using Engineering Sheet Ground Reference Data.

Subsection	From (mi)	To (mi)	HPMS Cracking Length (ft)			HPMS Cracking % (Wheel Path Width = 39 in)
			LWP	RWP	Total	
1	0.00	0.03	20	153	173	34
2	0.03	0.06	71	118	189	38
3	0.06	0.09	43	97	141	28
4	0.09	0.12	116	154	270	54
5	0.12	0.15	70	140	210	42
6	0.15	0.18	184	150	334	66
7	0.18	0.21	123	69	192	38
8	0.21	0.24	137	157	294	58
9	0.24	0.27	122	138	260	52
10	0.27	0.30	80	119	199	40
Total	0.00	0.30	966	1295	2261	45

Table 14. HPMS Cracking Percentage in 0.03 Mile Sections Using Testing System Data.

Subsection	From (mi)	To (mi)	HPMS Cracking Length (ft)			HPMS Cracking % (Wheel Path Width = 39 in)
			LWP	RWP	Total	
1	0.00	0.03	2.44	1.43	1.87	0.67
2	0.03	0.06	3.98	4.63	8.6	1.49
3	0.06	0.09	1.51	0	1.51	0.29
4	0.09	0.12	0.49	3.46	3.95	0.68
5	0.12	0.15	0.16	1.04	1.2	0.21
6	0.15	0.18	7.51	1.55	9.06	1.57
7	0.18	0.21	12.05	0.05	12.1	2.09
8	0.21	0.24	11.08	3.88	14.96	2.59
9	0.24	0.27	29.71	0.8	30.5	5.29
10	0.27	0.30	18.85	0	18.85	3.27
Total	0.00	0.30	87.86	16.85	104.61	1.81

5.2 Decomposed Methods Validation

Compared to the ground reference cracking annotation, the testing system provided crack map is assessed to have a performance EHD score of 34.45 (where the EHD ranges from 0 to 100, with 0 indicating poor alignment and 100 indicating perfect alignment), which indicates a moderate level of alignment between the detected crack map and the ground reference.

To better understand potential issues of vendor's crack measurement, the following two methods aim to decompose these issues into 1) sensor issues (e.g., image quality) or 2) crack detection issues.

5.2.1 Sensor Quality Evaluation Using Ground Reference Boards

This method uses known objects (i.e., ground reference boards) to evaluate the sensor quality, which was developed in NCHRP 01-60 and mentioned in Phase 1 (refer to the Phase 1 interim report Ch. 3.4). During the field data collection with FDOT in December 2024, we collected data of ground reference boards, as shown in **Figure 28**.

The details of this method were described in NCHRP 01-60. However, this method requires the raw range of data collected from the testing systems to be accurately evaluated. The current data we have is inaccessible from the testing system used in the FDOT field trip, which hinders the reproduction of such evaluation.

Despite the quantitative method, the data quality is evaluated using the qualitative visual inspection of the data collected from the ground reference boards. From the range image shown in **Figure 28 (c)**. Only a portion of the boards' texture is visible, possibly leading to the crack detection issue.

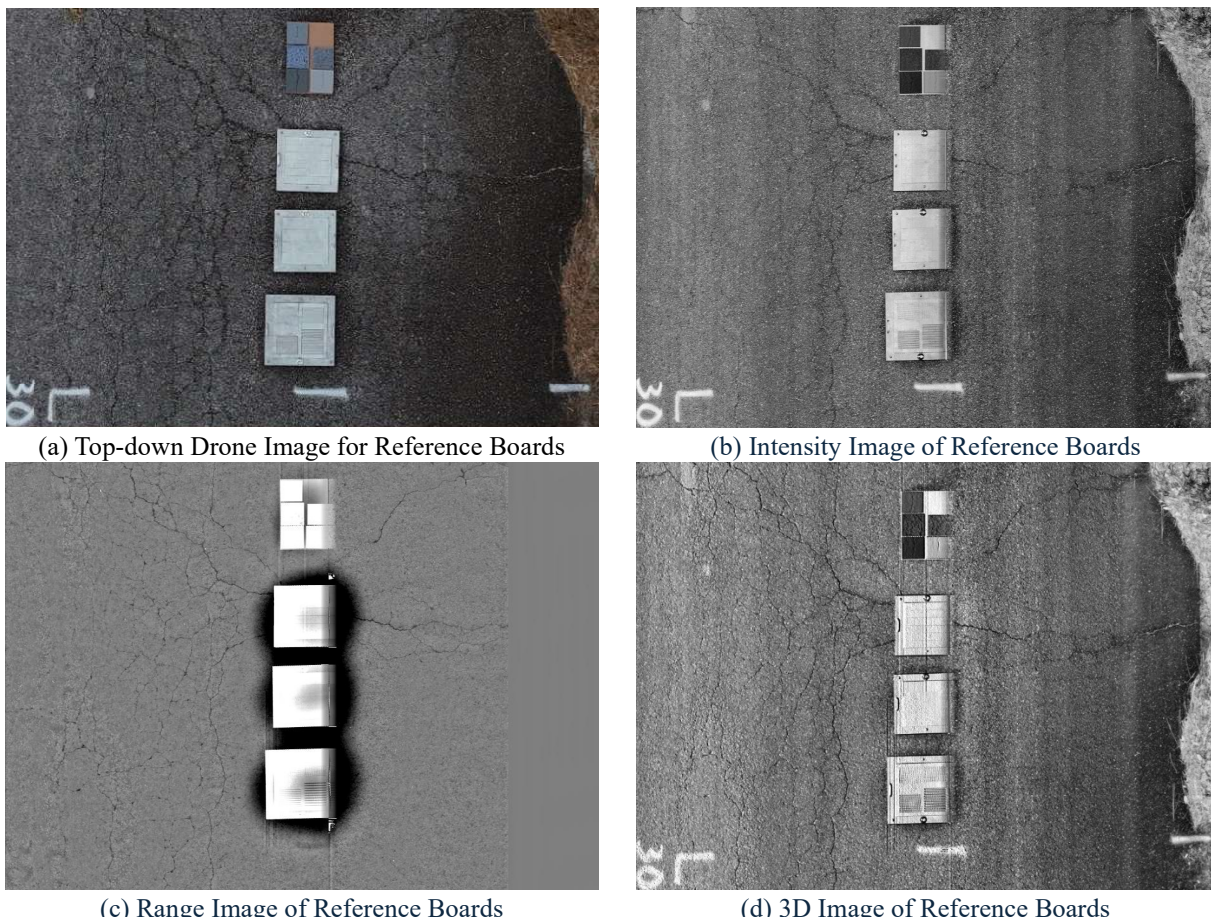


Figure 28. Data Collected from Testing System on Ground Reference Boards.

5.2.2 Crack Detection Accuracy Evaluation Using Inter-Rater Annotation

To evaluate the crack detection accuracy of the testing system, the ground referencing crack maps generated by manual annotation are used. The annotation used undergoes the inter-rater consensus and could represent the most accurate crack detection result that could be generated from the pavement images. The evaluation is conducted by calculating and analyzing the EHD scores between the testing system's

crack detection and the ground referencing crack map. **Figure 29** shows an example of the data used in the crack detection accuracy evaluation: **(a)** is the range image used for manual annotation and crack detection, **(b)** is the manual annotation results with red pixels representing cracks, and **(c)** is the binary crack map generated by the testing system with white pixels representing cracks.

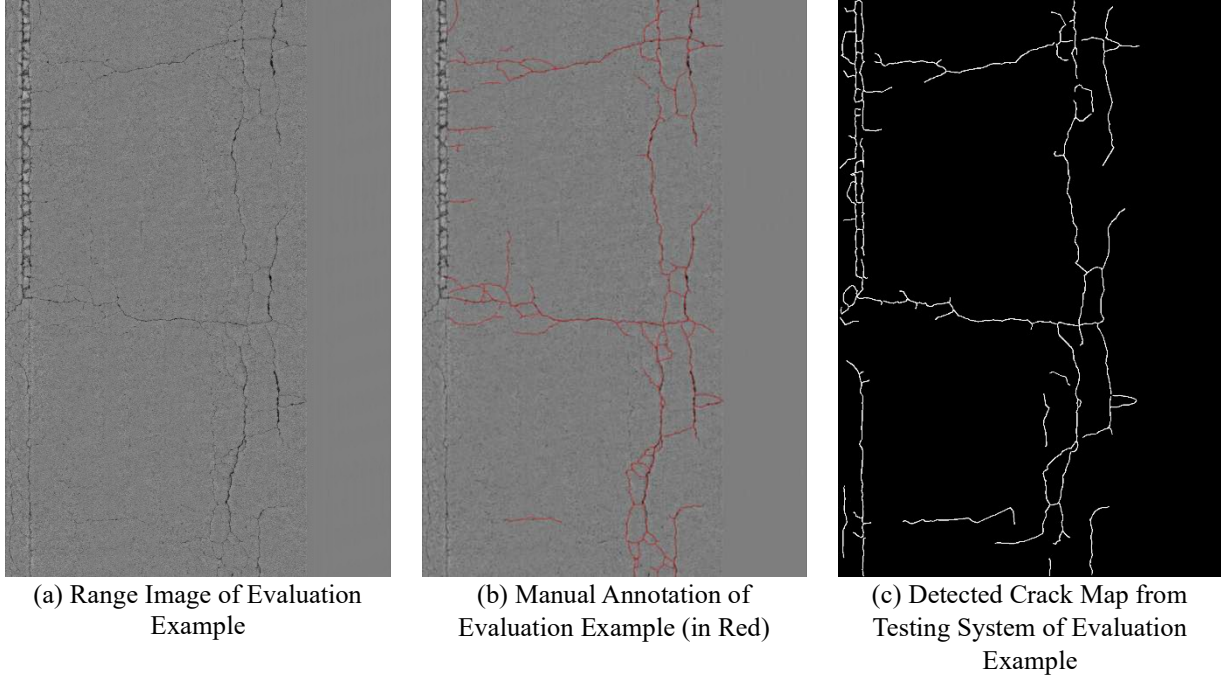


Figure 29. Example for Crack Detection Accuracy Evaluation.

The EHD results of **Figure 30** corresponding sections are:

- Performance Score: 47.41
- FP Penalty (False Positive Penalty): 0.53
- FN Penalty (False Negative Penalty): 0.52

The performance score of 47.41 indicates a moderate level of alignment between the detected crack map and the ground reference. The false positive penalty of 0.53 is largely due to the detection of cracks outside of the lane marking (as shown in red pixels in the upper part of **Figure 30 (c)**), which is acceptable as the cracks outside the lane marking will not impact the further crack information analysis. On the other hand, the false negative penalty of 0.52 indicates that a notable portion of actual crack pixels in the ground reference is missed (as shown in green pixels in the **Figure 30 (c)**), which illustrates that the testing system's detection algorithm has limitations in short and thin cracks, which are major components of the alligator cracks.

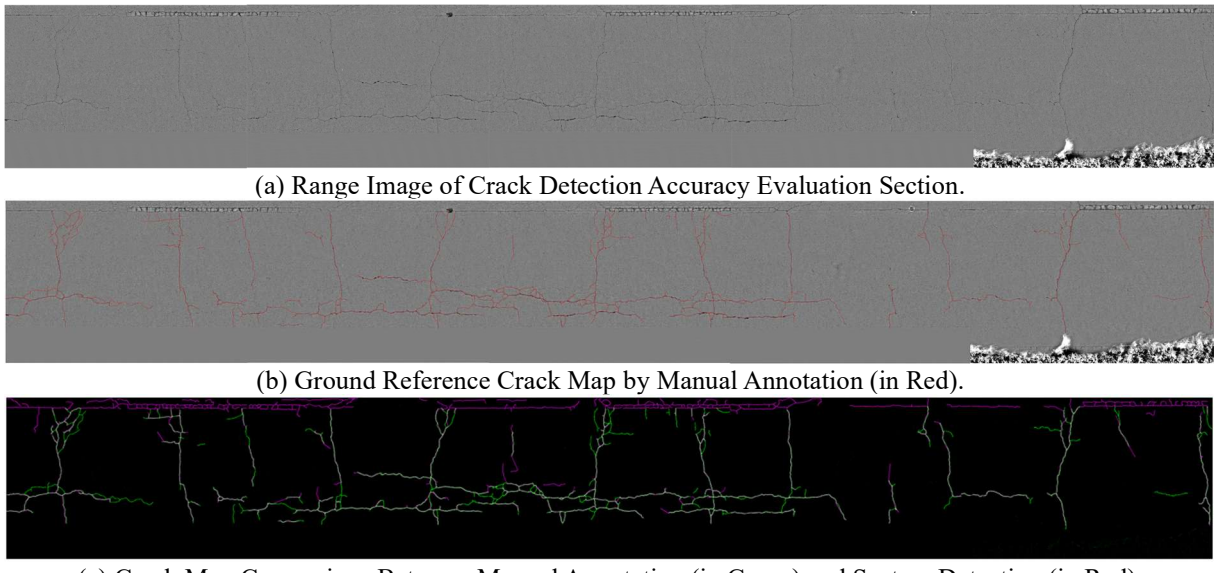


Figure 30. Case Study Section with Different Types of Crack Maps

As illustrated in the comparison between **Figure 25** and **Figure 30**, the detected crack map from the testing system aligns better with the manual crack map annotation than with the manual crack augmentation. A detailed visual comparison of the two sets of figures shows that the discrepancy stems from the invisibility of fine cracks in the range images that can be identified and augmented in the field. This conclusion aligns with the results of sensor quality challenges identified in **Section 5.2.1**.

6 Conclusion

The preliminary conclusions of Task 8 data analysis are listed below.

- 1) The feasibility of implementing the revised WOD-288 has been validated through the process of development and algorithms running.
- 2) Challenges and potential issues have been identified during the validation; key issues have been documented in **Section 2.5**.
- 3) Suggestions for further refining the cracking definition corresponding to the identified challenges have been made, and key suggestions have been summarized in **Section 2.6**.
- 4) Reporting HPMS cracking percentages using the revised WOD-288 has been examined and found feasible for SHAs' data, although the HPMS definition remains unclear for producing comparable results. We are collaborating with SHAs to cross-check the HPMS cracking percentage results and identify any necessary refinements.
- 5) Sensitivity studies have been made, showing a) the impact of grid size and location exists, b) most crack widths are 2–6 mm measured from pavement images collected from existing imaging systems, c) 0-20 and 70-90 degrees for splitting the transverse and longitudinal crack are reasonable.
- 6) The proposed data quality assessment method has also been examined using real-world data. The manual surface crack mapping (on the engineering sheet) method lacks detailed crack maps

(alligator/patterned cracking is only delineated by area), so to prove, it cannot identify the missing cracking detection on the testing system's image. Also, when crack density is relatively high, completing an engineering sheet survey on a 0.3-mile pavement section is difficult in 3 hours.

- 7) The manual cracking augmentation (on pavement surface) method is demonstrated to be an efficient way to quantify the percentage of cracks detected by the automated cracking measurement system. It is suggested to set up the testing section for 15 meters (~50 ft), so complicated cracking patterns, including 50% alligator cracking, can be completed within 3 hours (may need three raters to work together).
- 8) Through the field testing, the procedures for setting up the two end-to-end methods (i.e., engineering sheet survey method and cracking augmentation method) have been refined. The best practices can be introduced in detail for the standard development in the next tasks.

As mentioned, this report is a preliminary document that will be further refined in Task 9 – preparing a final report presenting the results of the work plan.

7 Appendix

7.1 Additional Results of Crack Width Distribution

It is important to note that the categories of cracking images are classified based on the predominant cracks in the selected images. While transverse cracking images may include longitudinal cracks, and vice versa, the selection of images is based on the dominant crack type.

- **Longitudinal Crack**

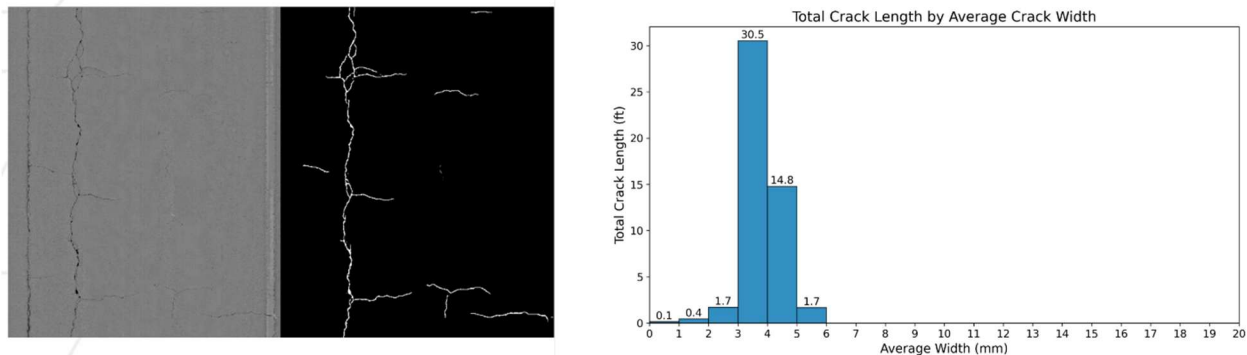


Figure 31. Example of crack width distribution for the longitudinal crack map (#611)

- **Transverse Crack**

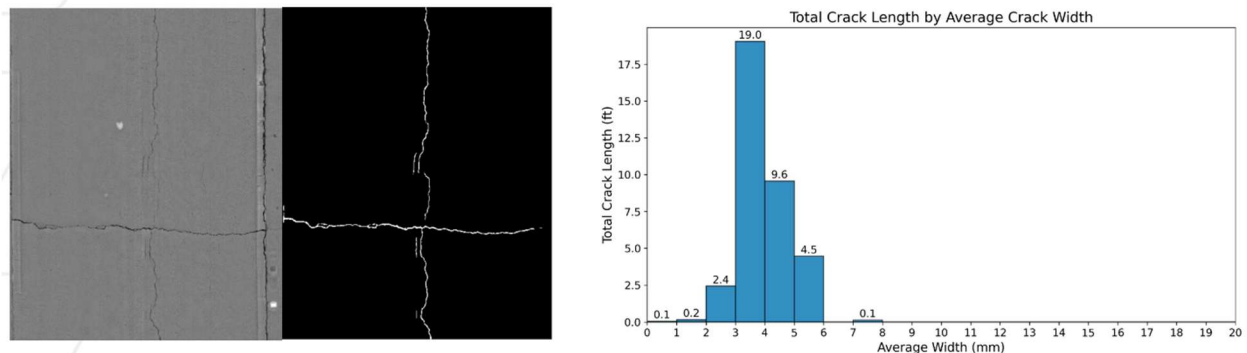


Figure 32. Example of crack width distribution for the transverse crack map (#286)

e) Block Crack

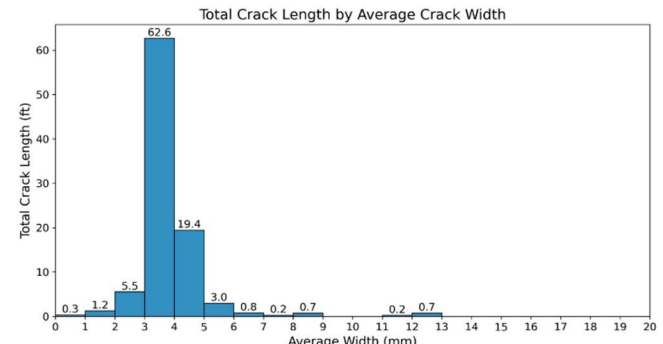
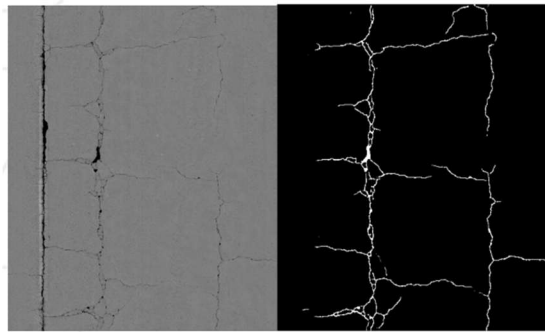


Figure 33. Example of crack width distribution for the block-cracking map (#450)

• Alligator Crack

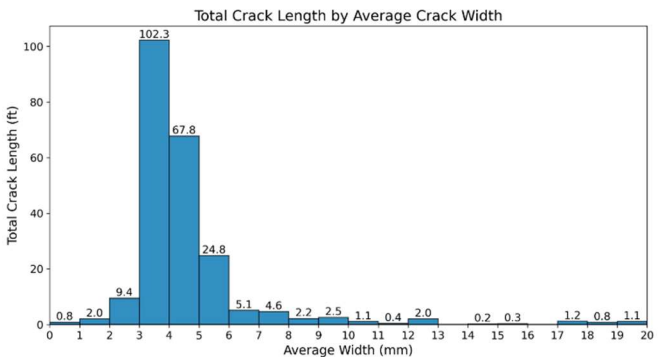
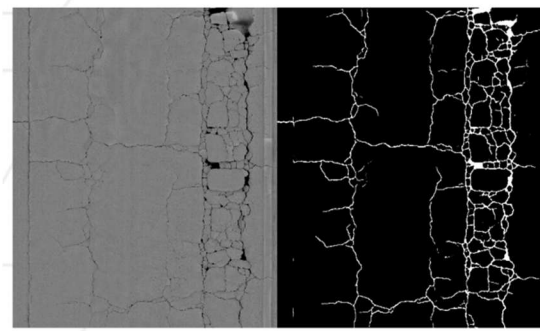


Figure 34. Example of crack width distribution for the alligator crack map (#872)

7.2 Additional Results of Crack Orientation Distribution Analysis

- **Longitudinal Crack**

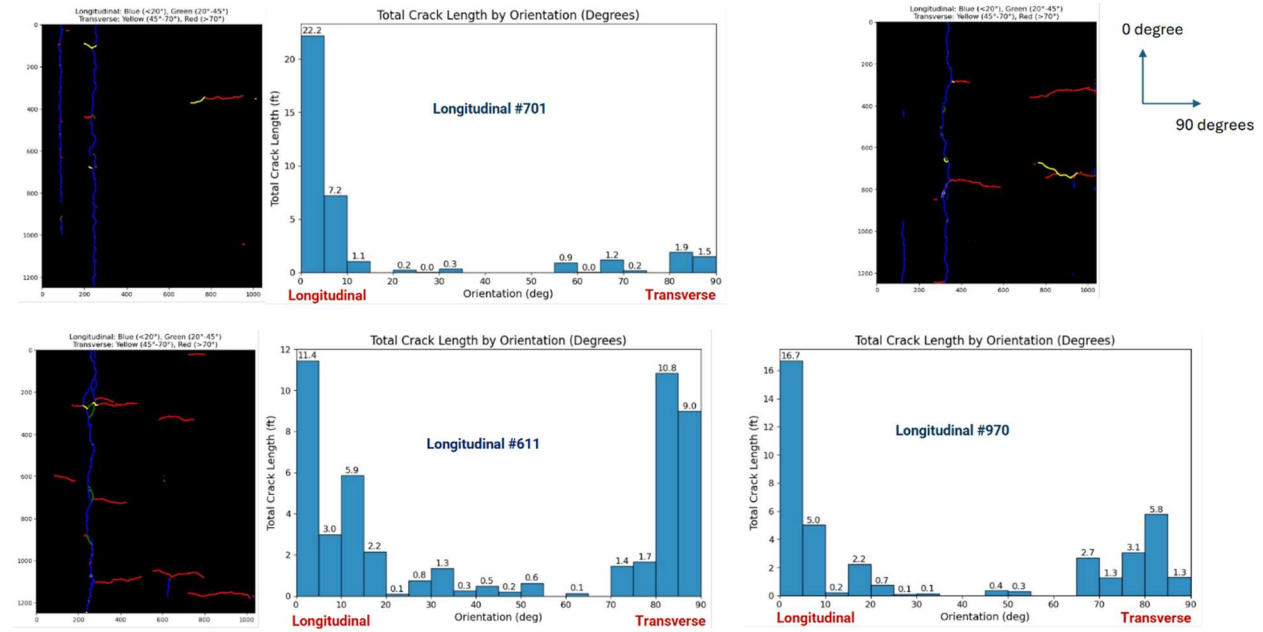


Figure 35. Examples of crack orientation distribution for longitudinal crack maps.

- **Transverse Crack**

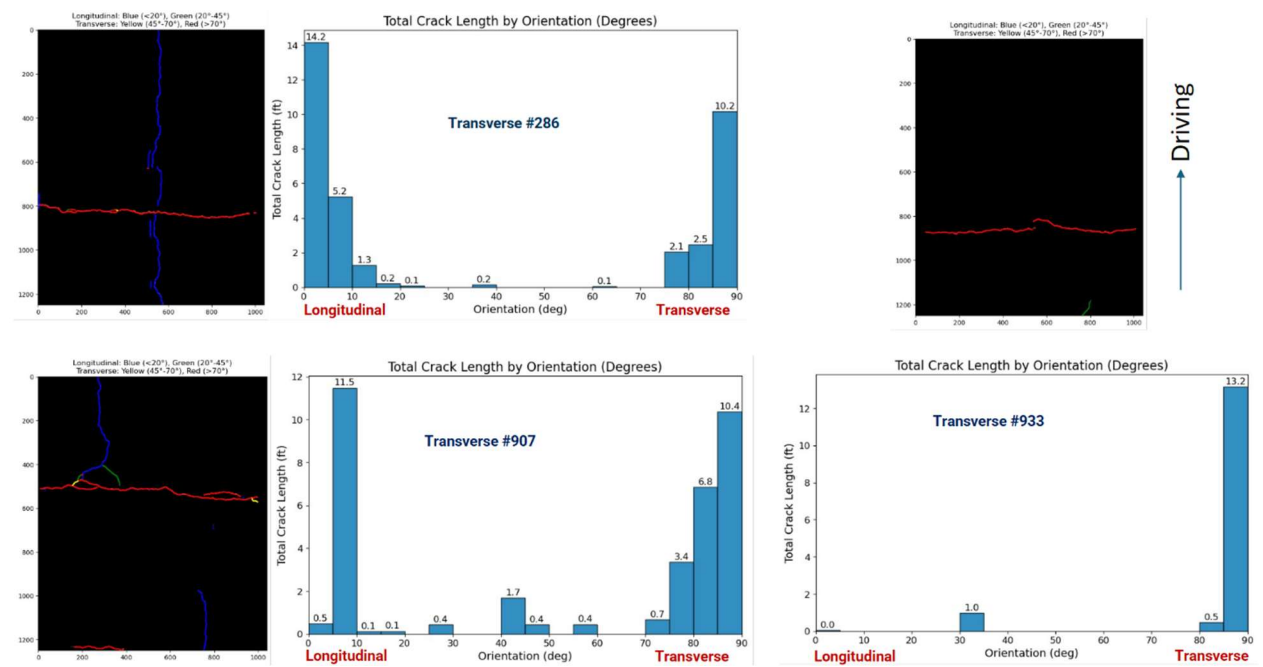


Figure 36. Examples of crack orientation distribution for transverse crack maps.

- **Block Crack**

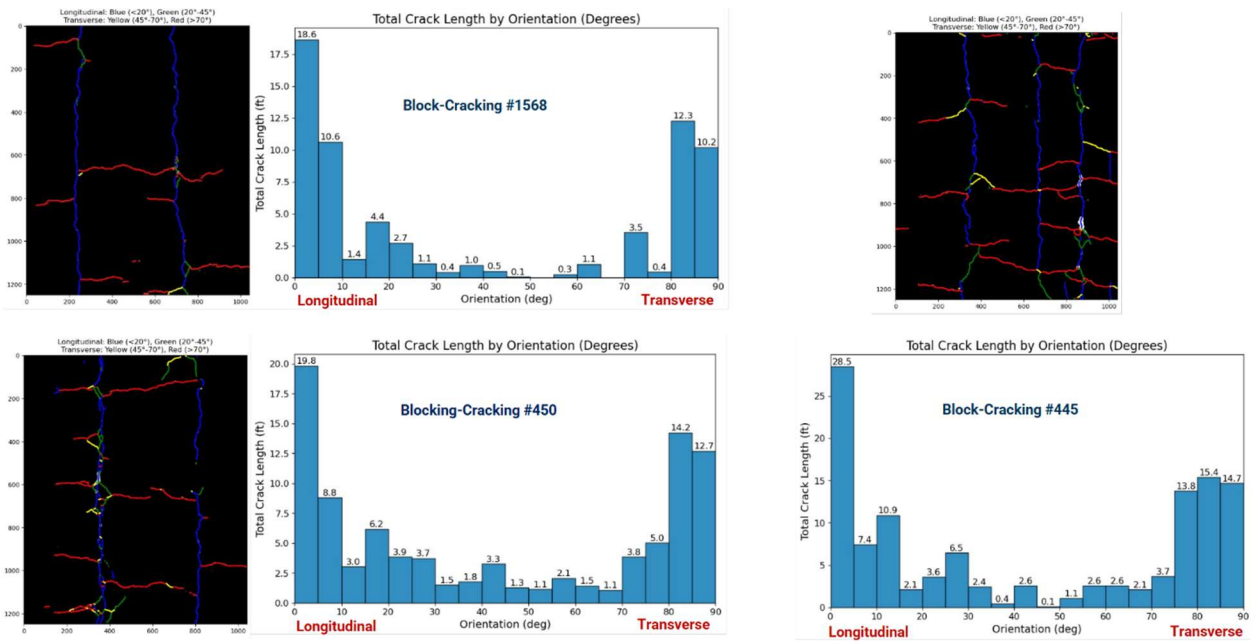


Figure 37. Examples of crack orientation distribution for block-cracking maps.

- **Alligator Crack**

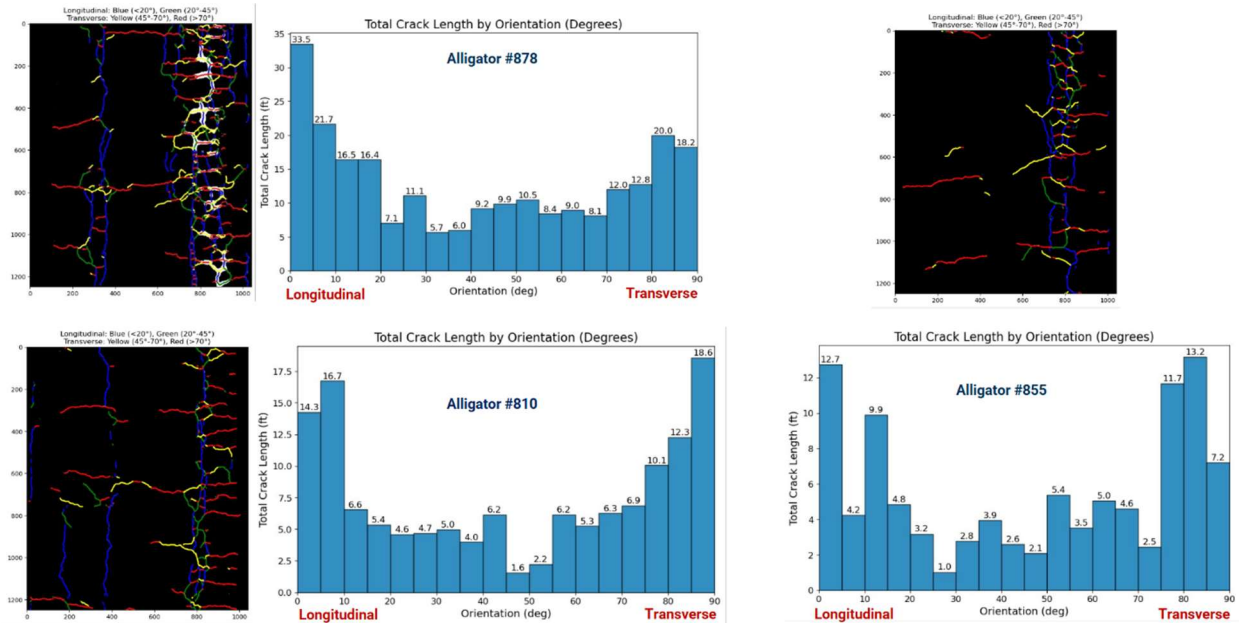


Figure 38. Examples of crack orientation distribution for alligator-cracking maps.

8 References

- FHWA. (2016). *Highway Performance Monitoring System Field Manual*.
<https://www.fhwa.dot.gov/policyinformation/hpms/fieldmanual/page06.cfm#toc249159741>
- Geary, G. M. (2019). A spatial and temporal 3D slab-based methodology for optimized concrete pavement asset management.
- Hsieh, Y.-A. (2023). *PAVEMENT CRACK SEGMENTATION WITH DENSE LOCAL GEOMETRY FEATURES AND BOUNDARY ENHANCEMENT LOSS* Georgia Institute of Technology].
- Hsieh, Y.-A., & Tsai, Y. J. (2020). Machine learning for crack detection: Review and model performance comparison. *Journal of Computing in Civil Engineering*, 34(5), 04020038.
- Hsieh, Y. A., Yang, Z., & James Tsai, Y. C. (2021). Convolutional neural network for automated classification of jointed plain concrete pavement conditions. *Computer - Aided Civil and Infrastructure Engineering*, 36(11), 1382-1397.
- Wang, K. C., Li, J. Q., & Yang, G. (2020). Standard Definitions for Common Types of Pavement Cracking. *NCHRP Web-Only Document*(NCHRP Project 01-57A).
- Yang, Z. (2024). *CRACK PROPAGATION ANALYSIS USING PAVEMENT IMAGE REGISTRATION AND CRACK VECTOR MODEL FOR PREDICTIVE AND PRECISION PAVEMENT MAINTENANCE* Georgia Institute of Technology].
- Yang, Z., Flynt, T., Salameh, R., Geary, G., & Tsai, Y.-C. (2025). Automated and Interpretable Classification of Jointed Plain Concrete Pavement (JPCP) Slab State Using Crack Vector Model (CVM). (*under preparation*).